

# $\lambda$ and $\rho$ Regge trajectories for hidden bottom and charm tetraquarks $(Qq)(\bar{Q}\bar{q}')$

Jia-Qi Xie,<sup>1,\*</sup> He Song,<sup>1,†</sup> Xia Feng,<sup>1,‡</sup> and Jiao-Kai Chen<sup>1,§</sup>

<sup>1</sup>*School of Physics and Information Engineering,  
Shanxi Normal University, Taiyuan 030031, China*

We propose the Regge trajectory relations for the heavy tetraquarks  $(Qq)(\bar{Q}\bar{q}')$  ( $Q = b, c; q, q' = u, d, s$ ) with hidden bottom and charm. By employing the new relations, both the  $\lambda$ -trajectories and the  $\rho$ -trajectories for the tetraquarks  $(Qq)(\bar{Q}\bar{q}')$  can be discussed. The masses of the  $\lambda$ -mode excited states and the  $\rho$ -mode excited states are estimated, and they agree with other theoretical predictions. We show that the behaviors of the  $\rho$ -trajectories are different from those of the  $\lambda$ -trajectories. The  $\rho$ -trajectories behave as  $M \sim x_\rho^{1/2}$  ( $x_\rho = n_r, l$ ) while the  $\lambda$ -trajectories behave as  $M \sim x_\lambda^{2/3}$  ( $x_\lambda = N_r, L$ ). Moreover, the Regge trajectory behaviors for other types of tetraquarks are investigated based on the spinless Salpeter equation. We show that both the  $\lambda$ -trajectories and the  $\rho$ -trajectories are concave downward in the  $(M^2, x)$  plane. The Regge trajectories for the tetraquarks containing the light diquark and/or the light antidiquark also are concave in the  $(M^2, x)$  plane when the masses of the light constituents are included and the confining potential is linear.

Keywords:  $\lambda$ -trajectory,  $\rho$ -trajectory, tetraquark, mass

## I. INTRODUCTION

As a type of exotic hadrons, tetraquarks will enhance the study of hadrons and will provide new probes for the understanding of QCD [1–8]. The heavy tetraquarks  $(Qq)(\bar{Q}\bar{q}')$  ( $Q = b, c; q, q' = u, d, s$ ) with hidden bottom and charm have been studied through various methods. These approaches include the relativistic quark model based on the quasipotential approach in QCD [9–11], the non-relativistic potential model [12, 13], the spinless Salpeter equation [14, 15], the relativistic four-body Faddeev-Yakubovsky equation [16], the dynamical diquark model [17–20], the homogeneous Lippmann-Schwinger integral equation [21], the effective Hamiltonian in the adopted chromomagnetic interaction model [22], the chiral quark model [23], the sum rules [24, 25], the relativistic four-quark equations in the framework of coupled-channel formalism [26], the constituent quark model [27], among others.

The Regge trajectory<sup>1</sup> is one of the effective approaches widely used in the study of hadron spectra [35–41]. Ref. [42] gives a compact and predictive unified picture of mesons, baryons, and tetraquarks with the loaded flux-tube model. Ref. [43] presents relations between the

Regge trajectories of mesons, baryons, and tetraquarks based on the Holographic light front QCD. In Ref. [44], the masses of mesons, baryons, glueballs, and tetraquarks are predicted by the Regge trajectories obtained from the holography inspired stringy hadron model. In Ref. [45], mesons, hybrid mesons and multiquark states are discussed by the nonlinear Regge trajectories in the model AdS/QCD with dilaton. In Refs. [33, 34], we discuss the universal descriptions of the heavy-heavy and heavy-light systems by using the Regge trajectories. In preceding works, the Regge trajectories for the tetraquarks are the  $\lambda$ -trajectories. To our knowledge, no studies address the  $\rho$ -trajectories for tetraquarks although there are many studies on the  $\rho$ -excited states of tetraquarks. In the diquark picture, the hidden bottom tetraquarks are composed of one heavy-light diquark ( $Qq$ ) and one heavy-light antidiquark ( $\bar{Q}\bar{q}'$ ). By applying the Regge trajectory relation for the heavy-light diquarks [29] and the Regge trajectory formula for the heavy-heavy systems [34], we present the Regge trajectory relations for the hidden bottom and charm tetraquarks. The masses of the  $\lambda$ -mode excited and  $\rho$ -mode excited tetraquarks with hidden bottom and charm are estimated. Both the  $\lambda$ -trajectories and  $\rho$ -trajectories are investigated.

The paper is organized as follows: In Sec. II, the Regge trajectories for the hidden bottom and charm tetraquarks are discussed. The conclusions are presented in Sec. III. The discussions on the Regge trajectory behaviors for various tetraquarks are in the appendix C.

## II. REGGE TRAJECTORIES FOR THE TETRAQUARKS WITH HIDDEN BOTTOM AND CHARM

In this section, with the help of the diquark Regge trajectories [29, 46, 47], we investigate the Regge trajectory behaviors for various tetraquarks. The Regge trajectory relations are presented, which can be employed to discuss

\*Electronic address: 1462718751@qq.com

†Electronic address: songhe\_22@163.com

‡Electronic address: sxsdwxfx@163.com

§Electronic address: chenjk@sxnu.edu.cn, chenjkphy@outlook.com  
(corresponding author)

<sup>1</sup> A Regge trajectory of hadrons is assumed to be written as  $M = m_R + \beta_x(x + c_0)^\nu$  ( $x = l, n_r$ ), where  $M$  is mass of the bound state,  $l$  is the orbital angular momentum, and  $n_r$  is the radial quantum number.  $m_R$  and  $\beta_x$  are parameters. For simplicity, the plots in the  $(M, x)$  plane [28, 29], in the  $(M, (x - c_0)^\nu)$  plane [30], in the  $(M^2, x)$  plane [31, 32], in the  $((M - m_R)^2, x)$  plane [33, 34] or in the  $((M - m_R)^{1/\nu}, x)$  plane [see Fig. 6 in this work] are all called the Chew-Frautschi plots. The Regge trajectories can be plotted in these different planes.

both the  $\lambda$ -trajectories and the  $\rho$ -trajectories.

### A. Preliminary

In the diquark picture, tetraquarks consist of one diquark and one antidiquark, see Fig. 1.  $\rho_1$  ( $\rho_2$ ) separates the quarks (antiquarks) in the diquark (antidiquark), and  $\lambda$  separates the diquark and the antidiquark. There exist three excited modes: the  $\rho_1$ -mode involves the radial and orbital excitation in the diquark, the  $\rho_2$ -mode involves the radial and orbital excitation in the antidiquark, and the  $\lambda$ -mode involves the radial or orbital excitation between the diquark and antidiquark. Consequently, there exist three series of Regge trajectories: two series of  $\rho$ -Regge trajectories and one series of  $\lambda$ -Regge trajectories.

In  $SU_c(3)$ , there is attraction between quark pairs ( $qq'$ ) in the color antitriplet channel and this is just twice weaker than in the color singlet  $q\bar{q}'$  in the one-gluon exchange approximation. Only the  $\bar{3}_c$  representation of  $SU_c(3)$  is considered in the present work; the  $6_c$  representation is not considered. The tetraquarks considered are composed of a diquark and an antidiquark in color  $\bar{3}$  and 3 configuration.

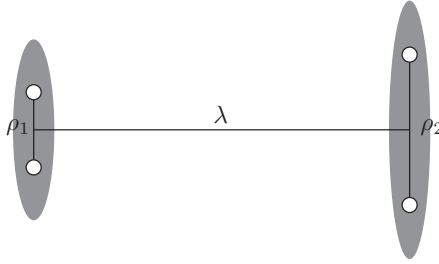


FIG. 1: Schematic diagram of the tetraquarks in the diquark-antidiquark picture.

In the diquark picture, the state of tetraquark is denoted as

$$\left( (q_1 q'_1)^{\bar{3}_c}_{n_1^{2s_1+1} l_{1j_1}} (\bar{q}_2 \bar{q}'_2)^{3_c}_{n_2^{2s_2+1} l_{2j_2}} \right)^{1_c}_{N^{2j+1} L_J}, \quad (1)$$

where  $\bar{3}_c$  denotes the color antitriplet state of diquark, and  $1_c$  represents the color singlet state of tetraquark. [The superscript  $1_c$  is often omitted because the tetraquarks are colorless.] The diquark ( $q_1 q'_1$ ) is  $\{q_1 q'_1\}$  or  $[q_1 q'_1]$ . The antidiquark ( $\bar{q}_2 \bar{q}'_2$ ) is  $\{\bar{q}_2 \bar{q}'_2\}$  or  $[\bar{q}_2 \bar{q}'_2]$ .  $\{qq'\}$  and  $[qq']$  indicate the permutation symmetric and antisymmetric flavor wave functions, respectively.  $N = N_r + 1$ , where  $N_r = 0, 1, \dots$ .  $n_{r1,2} = n_{r_{1,2}} + 1$ , where  $n_{r_{1,2}} = 0, 1, \dots$ .  $N_r$ ,  $n_{r1}$  and  $n_{r2}$  are the radial quantum numbers of the tetraquark, diquark 1, antidiquark 2, respectively. The completely antisymmetric states for the diquarks in  $\bar{3}_c$  are listed in Table IX.  $\vec{J} = \vec{L} + \vec{j}$ ,  $\vec{j} = \vec{j}_1 + \vec{j}_2$ ,  $\vec{j}_1 = \vec{s}_1 + \vec{l}_1$ ,  $\vec{j}_2 = \vec{s}_2 + \vec{l}_2$ .  $\vec{J}$ ,  $\vec{j}_1$  and  $\vec{j}_2$  are the spins of tetraquark, diquark 1, antidiquark 2, respectively.  $\vec{j}$

is the summed spin of diquarks and antidiquarks in the tetraquark.  $L$ ,  $l_1$  and  $l_2$  are the orbital quantum numbers of tetraquark, diquark 1 and antidiquark 2, respectively.  $\vec{s}_1$  ( $\vec{s}_2$ ) is the summed spin of quarks (antiquarks) in the diquark (antidiquark).

### B. Regge trajectory relations for the hidden bottom and charm tetraquarks

The tetraquarks with hidden bottom and charm consists of one heavy-light diquark ( $Qq$ ) and one heavy-light antidiquark ( $\bar{Q}\bar{q}'$ ). Both ( $Qq$ ) and ( $\bar{Q}\bar{q}'$ ) are heavy because the bottom/charm quark are heavy. Therefore, the tetraquarks ( $Qq$ )( $\bar{Q}\bar{q}'$ ) are the heavy-heavy systems in case of the  $\lambda$ -mode excitations. Meanwhile, the Regge trajectories for ( $Qq$ )( $\bar{Q}\bar{q}'$ ) exhibit the properties of the heavy-light systems in case of the  $\rho$ -mode excitations. According to Eqs. (C31) and (C32), we list the relations for the tetraquarks with hidden bottom and charm

$$\begin{aligned} M &= m_{R\lambda} + \beta_{x_\lambda} (x_\lambda + c_{0x_\lambda})^{2/3} \quad (x_\lambda = L, N_r), \\ M_{\rho_1} &= m_{R\rho_1} + \beta_{x_{\rho_1}} \sqrt{x_{\rho_1} + c_{0x_{\rho_1}}} \quad (x_{\rho_1} = l_1, n_{r1}), \\ M_{\rho_2} &= m_{R\rho_2} + \beta_{x_{\rho_2}} \sqrt{x_{\rho_2} + c_{0x_{\rho_2}}} \quad (x_{\rho_2} = l_2, n_{r2}), \end{aligned} \quad (2)$$

where

$$\begin{aligned} m_{R\lambda} &= M_{\rho_1} + M_{\rho_2} + C, \\ m_{R\rho_1} &= m_Q + m_q + C/2, \\ m_{R\rho_2} &= m_Q + m_{q'} + C/2, \\ \beta_L &= \frac{3}{2} \left( \frac{\sigma^2}{\mu_\lambda} \right)^{1/3} c_{fL}, \\ \beta_{N_r} &= \frac{(3\pi)^{2/3}}{2} \left( \frac{\sigma^2}{\mu_\lambda} \right)^{1/3} c_{fN_r}, \\ \mu_\lambda &= \frac{M_{\rho_1} M_{\rho_2}}{M_{\rho_1} + M_{\rho_2}}, \\ \beta_{l_1} &= \sqrt{2\sigma} c_{fl_1}, \quad \beta_{n_{r1}} = \sqrt{\pi\sigma} c_{fn_{r1}}, \\ \beta_{l_2} &= \sqrt{2\sigma} c_{fl_2}, \quad \beta_{n_{r2}} = \sqrt{\pi\sigma} c_{fn_{r2}}. \end{aligned} \quad (3)$$

$M$ ,  $M_{\rho_1}$ ,  $M_{\rho_2}$ ,  $m_Q$ , and  $m_q$  are the tetraquark mass, the diquark mass, the antidiquark mass, the heavy quark mass, and the light quark mass, respectively.  $\sigma$  is the string tension.  $C$  is a fundamental parameter.  $c_{fx}$  are theoretically equal to one but are fitted in practice.  $c_{0x}$  vary with Regge trajectories.

### C. Parameters

The quark masses, the string tension  $\sigma$  and the parameter  $C$  are from Ref. [10]. The parameters for the heavy-light diquarks ( $bu$ ), ( $bs$ ), ( $cu$ ), and ( $cs$ ) are from Ref. [29] and listed in Table I. With these parameters determined, the  $\rho$ -modes and the diquark masses can be discussed, see Eqs. (2) and (3). To discuss the masses

of the hidden bottom and charm tetraquarks and the  $\lambda$ -modes excited states, the parameters  $c_{fL}$ ,  $c_{fN_r}$ ,  $c_{0L}$  and  $c_{0N_r}$  should be determined, see Eqs. (D2) and (D3). More discussions are in section D. Once all parameters are determined, the Regge trajectories can be discussed and can be used to estimate the masses of the tetraquarks with hidden bottom and charm.

TABLE I: The values of parameters [10, 29].

	$m_{u,d} = 0.33 \text{ GeV}$ , $m_s = 0.50 \text{ GeV}$ , $m_b = 4.88 \text{ GeV}$ $m_c = 1.55 \text{ GeV}$ , $\sigma = 0.18 \text{ GeV}^2$ , $C = -0.3 \text{ GeV}$
(bu)	$c_{fn_{r_1}} = c_{fn_{r_2}} = 0.988$ , $c_{fl_1} = c_{fl_2} = 0.965$ $c_{0n_{r_1}}(1^1s_0) = c_{0n_{r_2}}(1^1s_0) = 0.125$ $c_{0n_{l_1}}(1^1s_0) = c_{0n_{l_2}}(1^1s_0) = 0.18$ $c_{0n_{r_1}}(1^3s_1) = c_{0n_{r_2}}(1^3s_1) = 0.155$ $c_{0n_{l_1}}(1^3s_1) = c_{0n_{l_2}}(1^3s_1) = 0.22$
(bs)	$c_{fn_{r_1}} = c_{fn_{r_2}} = 0.953$ , $c_{fl_1} = c_{fl_2} = 0.919$ $c_{0n_{r_1}}(1^1s_0) = c_{0n_{r_2}}(1^1s_0) = 0.08$ $c_{0n_{l_1}}(1^1s_0) = c_{0n_{l_2}}(1^1s_0) = 0.115$ $c_{0n_{r_1}}(1^3s_1) = c_{0n_{r_2}}(1^3s_1) = 0.11$ $c_{0n_{l_1}}(1^3s_1) = c_{0n_{l_2}}(1^3s_1) = 0.16$
(cu)	$c_{fn_{r_1}} = c_{fn_{r_2}} = 1.000$ , $c_{fl_1} = c_{fl_2} = 1.038$ $c_{0n_{r_1}}(1^1s_0) = c_{0n_{r_2}}(1^1s_0) = 0.065$ $c_{0n_{l_1}}(1^1s_0) = c_{0n_{l_2}}(1^1s_0) = 0.095$ $c_{0n_{r_1}}(1^3s_1) = c_{0n_{r_2}}(1^3s_1) = 0.17$ $c_{0n_{l_1}}(1^3s_1) = c_{0n_{l_2}}(1^3s_1) = 0.19$
(cs)	$c_{fn_{r_1}} = c_{fn_{r_2}} = 1.016$ , $c_{fl_1} = c_{fl_2} = 1.015$ $c_{0n_{r_1}}(1^1s_0) = c_{0n_{r_2}}(1^1s_0) = 0.03$ $c_{0n_{l_1}}(1^1s_0) = c_{0n_{l_2}}(1^1s_0) = 0.055$ $c_{0n_{r_1}}(1^3s_1) = c_{0n_{r_2}}(1^3s_1) = 0.095$ $c_{0n_{l_1}}(1^3s_1) = c_{0n_{l_2}}(1^3s_1) = 0.135$

#### D. $\lambda$ - and $\rho$ -trajectories for the hidden bottom tetraquarks

The tetraquarks with hidden bottom include the neutral states  $(bu)(\bar{b}\bar{u})$  and  $(bd)(\bar{b}\bar{d})$ , the charged states  $(bu)(\bar{b}\bar{d})$  and  $(bd)(\bar{b}\bar{u})$ , the states with open strangeness  $(bs)(\bar{b}\bar{n})$  and  $(bn)(\bar{b}\bar{s})$  ( $n = u, d$ ), and the states with hidden strangeness  $(bs)(\bar{b}\bar{s})$ . We assume  $m_u = m_d$ , therefore, the masses for diquarks  $(bd)$  and  $(bu)$  are equal and it holds for the tetraquarks as well.

When calculating the  $\lambda$ -mode excitations, the scalar diquark and the scalar antidiquark are used. The radially and orbitally excited states of the  $\lambda$ -mode are calculated by using Eqs. (2), (D2) and (D3) and parameters in Table I. The calculated results are listed in Table II. More results can be easily obtained in a similar manner. The  $\lambda$ -trajectories for the hidden bottom tetraquarks are shown in Fig. 2.

As discussed in Section D, the values of  $c_{fx_\lambda}$  and  $c_{0x_\lambda}$  vary with the masses of diquark and antidiquark,  $M_{\rho_1}$  and  $M_{\rho_2}$ , see Eqs. (2), (D2) and (D3). This means that  $c_{fx_\lambda}$  and  $c_{0x_\lambda}$  vary with different states of diquark or antidiquark as we discuss the  $\rho$ -trajectories, even though

$\lambda$ -mode remains ground state. Using Eqs. (2), (D2) and (D3) and parameters in Table I, the masses of the  $\rho$ -mode excited states are calculated and listed in Table IV.

The mass of the state  $|n_1^{2s_1+1}l_{1j_1}, n_2^{2s_2+1}l_{2j_2}, N^{2j+1}L_J\rangle$  for  $(bq)(\bar{b}\bar{q}')$  is equal to that of the state  $|n_2^{2s_2+1}l_{2j_2}, n_1^{2s_1+1}l_{1j_1}, N^{2j+1}L_J\rangle$  for  $(bq')(\bar{b}\bar{q})$ . For the  $\rho$ -mode excited states, the mass of the state  $|n_1^{2s_1+1}l_{1j_1}, n_2^{2s_2+1}l_{2j_2}, N^{2j+1}L_J\rangle$  with definite parity and charge parity (for  $q = q'$ )  $1/\sqrt{2}[(bq)(\bar{b}\bar{q}') \pm (bq')(\bar{b}\bar{q})]$  is equal to that of state

$$\begin{aligned} & |n_1^{2s_1+1}l_{1j_1}, n_2^{2s_2+1}l_{2j_2}, N^{2j+1}L_J\rangle' \\ &= \frac{1}{\sqrt{2}} \left( |n_1^{2s_1+1}l_{1j_1}, n_2^{2s_2+1}l_{2j_2}, N^{2j+1}L_J\rangle \right. \\ &\quad \left. \pm |n_2^{2s_2+1}l_{2j_2}, n_1^{2s_1+1}l_{1j_1}, N^{2j+1}L_J\rangle \right) \end{aligned} \quad (4)$$

for  $(bq)(\bar{b}\bar{q}')$  if  $n_1^{2s_1+1}l_{1j_1}$  is not identical to  $n_2^{2s_2+1}l_{2j_2}$ . The corresponding masses should be  $M = (M' + M'')/2$ , where  $M'$  and  $M''$  are listed in Table IV. Therefore, the corresponding tetraquarks will be degenerate in mass. The  $\rho$ -trajectories are shown in Fig. 3.

The obtained results for the  $\lambda$ -mode excited states are in agreement with other theoretical predictions, see Table III. To our knowledge, the highly radially and orbitally excited states of the  $\lambda$ -mode states,  $|1^1s_0, 1^1s_0, 4^1S_0\rangle$ ,  $|1^1s_0, 1^1s_0, 5^1S_0\rangle$ ,  $|1^1s_0, 1^1s_0, 1^1F_3\rangle$ ,  $|1^1s_0, 1^1s_0, 1^1G_4\rangle$ ,  $|1^1s_0, 1^1s_0, 1^1H_5\rangle$ , and the  $\rho$ -trajectories of the hidden bottom and charm tetraquarks are discussed for the first time.

The observed  $T_{b\bar{b}1}(10610)^+$  has been investigated by various theoretical approaches, see Ref. [48] for references. If  $T_{b\bar{b}1}(10610)^+$  is a tetraquark, it is the possible candidate for the  $|1^3s_1, 1^1s_0, 1^3S_1\rangle'$  state or the  $|1^3s_1, 1^3s_1, 1^3S_1\rangle$  state, see Table V. The theoretical predictions agree with the experimental data.

#### E. $\lambda$ - and $\rho$ -trajectories for the hidden charm tetraquarks

The discussions on the hidden charm tetraquarks are the same as those on the hidden bottom tetraquarks. We assume  $m_u = m_d$ , therefore, the masses for diquarks  $(cd)$  and  $(cu)$  are equal and it holds for the tetraquarks as well.

When considering the  $\lambda$ -mode excitations, the scalar diquark and the scalar antidiquark are used. Employing Eqs. (2), (D2), (D3), and parameters in Table I, the masses of the  $\lambda$ -mode excited states are estimated, see Table VI. The obtained results for the  $\lambda$ -mode excited states are in agreement with other theoretical predictions, see Table VII. The  $\lambda$ -trajectories are shown in Fig. 4.

When considering the  $\rho$ -mode excited states, the  $\lambda$ -mode state is the ground state,  $L = 0$  and  $N_r = 0$ . The masses of the  $\rho$ -mode excited states are calculated, see Table VIII.

TABLE II: The masses of the  $\lambda$ -mode excited states of the hidden bottom tetraquarks (in GeV). The notation in Eq. (1) is rewritten as  $|n_1^{2s_1+1}l_{1j_1}, n_2^{2s_2+1}l_{2j_2}, N^{2j+1}L_J\rangle$ .  $n = u, d$ . Eqs. (2), (D2) and (D3) are used.

$ n_1^{2s_1+1}l_{1j_1}, n_2^{2s_2+1}l_{2j_2}, N^{2j+1}L_J\rangle$	$(bn)(\bar{b}\bar{n})$	$(bn)(\bar{b}\bar{s})$	$(bs)(\bar{b}\bar{s})$
$ 1^1s_0, 1^1s_0, 1^1S_0\rangle$	10.46	10.57	10.68
$ 1^1s_0, 1^1s_0, 2^1S_0\rangle$	10.91	11.02	11.12
$ 1^1s_0, 1^1s_0, 3^1S_0\rangle$	11.21	11.32	11.43
$ 1^1s_0, 1^1s_0, 4^1S_0\rangle$	11.47	11.57	11.68
$ 1^1s_0, 1^1s_0, 5^1S_0\rangle$	11.70	11.80	11.91
$ 1^1s_0, 1^1s_0, 1^1S_0\rangle$	10.46	10.57	10.68
$ 1^1s_0, 1^1s_0, 1^1P_1\rangle$	10.78	10.89	11.00
$ 1^1s_0, 1^1s_0, 1^1D_2\rangle$	11.01	11.12	11.22
$ 1^1s_0, 1^1s_0, 1^1F_3\rangle$	11.20	11.31	11.41
$ 1^1s_0, 1^1s_0, 1^1G_4\rangle$	11.37	11.48	11.59
$ 1^1s_0, 1^1s_0, 1^1H_5\rangle$	11.53	11.64	11.74

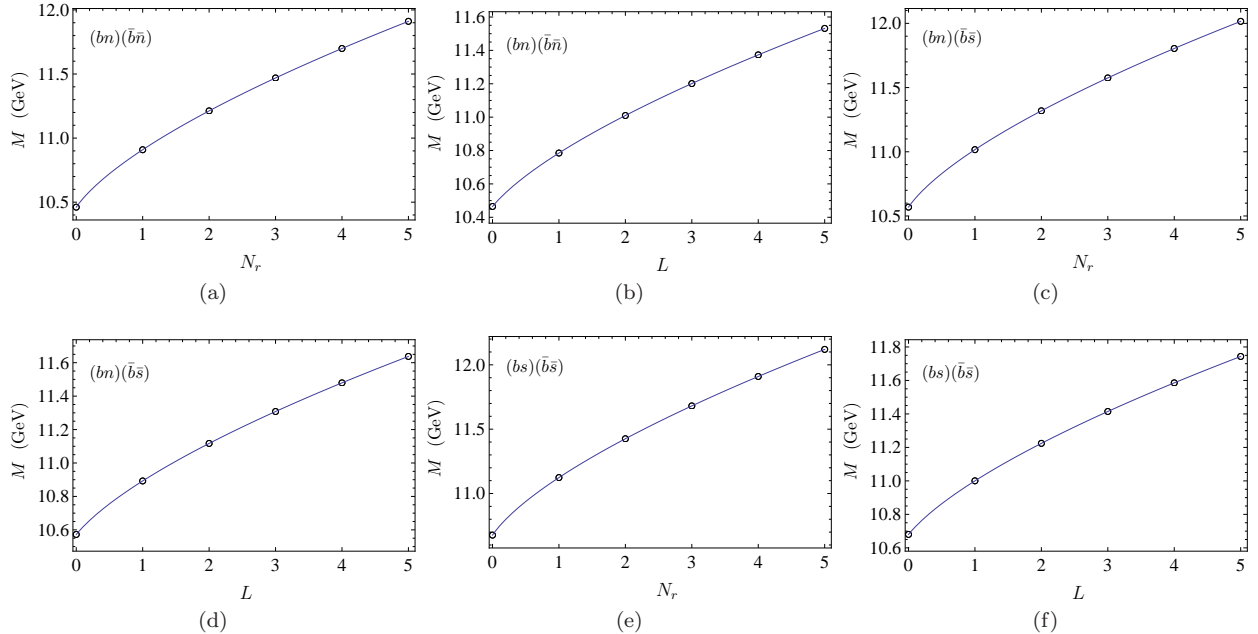


FIG. 2: The  $\lambda$ -trajectories for the hidden bottom tetraquarks. Circles represent the predicted data and the blue lines are the  $\lambda$ -trajectories, see Eq. (2). Data are listed in Table II.  $M$  is the bound state mass.  $N_r$  and  $L$  are the radial and orbital quantum numbers for the  $\lambda$ -mode, respectively.

TABLE III: Comparison of theoretical predictions for the masses of the hidden bottom tetraquarks (in GeV). The charge conjugation  $C$  is defined only for  $q = q'$ .

$J^{PC}$	$ n_1^{2s_1+1}l_{1j_1}, n_2^{2s_2+1}l_{2j_2}, N^{2j+1}L_J\rangle$	Tetraquark	Our	FGS [10]	FS [14]	TR [12]	HK [21]
$0^{++}$	$ 1^1s_0, 1^1s_0, 1^1S_0\rangle$	$(bn)(\bar{b}\bar{n})$	10.46	10.471			10.410
		$(bn)(\bar{b}\bar{s})$	10.57	10.572	10.407	10.522	
		$(bs)(\bar{b}\bar{s})$	10.68	10.662		10.711	10.613
	$ 1^1s_0, 1^1s_0, 2^1S_0\rangle$	$(bn)(\bar{b}\bar{n})$	10.91	10.917			10.899
		$(bn)(\bar{b}\bar{s})$	11.02	11.018	10.909	11.085	
		$(bs)(\bar{b}\bar{s})$	11.12	11.111		11.244	11.100
$1^{--}$	$ 1^1s_0, 1^1s_0, 1^1P_1\rangle$	$(bn)(\bar{b}\bar{n})$	10.78	10.807			10.806
		$(bn)(\bar{b}\bar{s})$	10.89	10.907	10.790	11.024	
		$(bs)(\bar{b}\bar{s})$	11.00	11.002		11.184	11.009

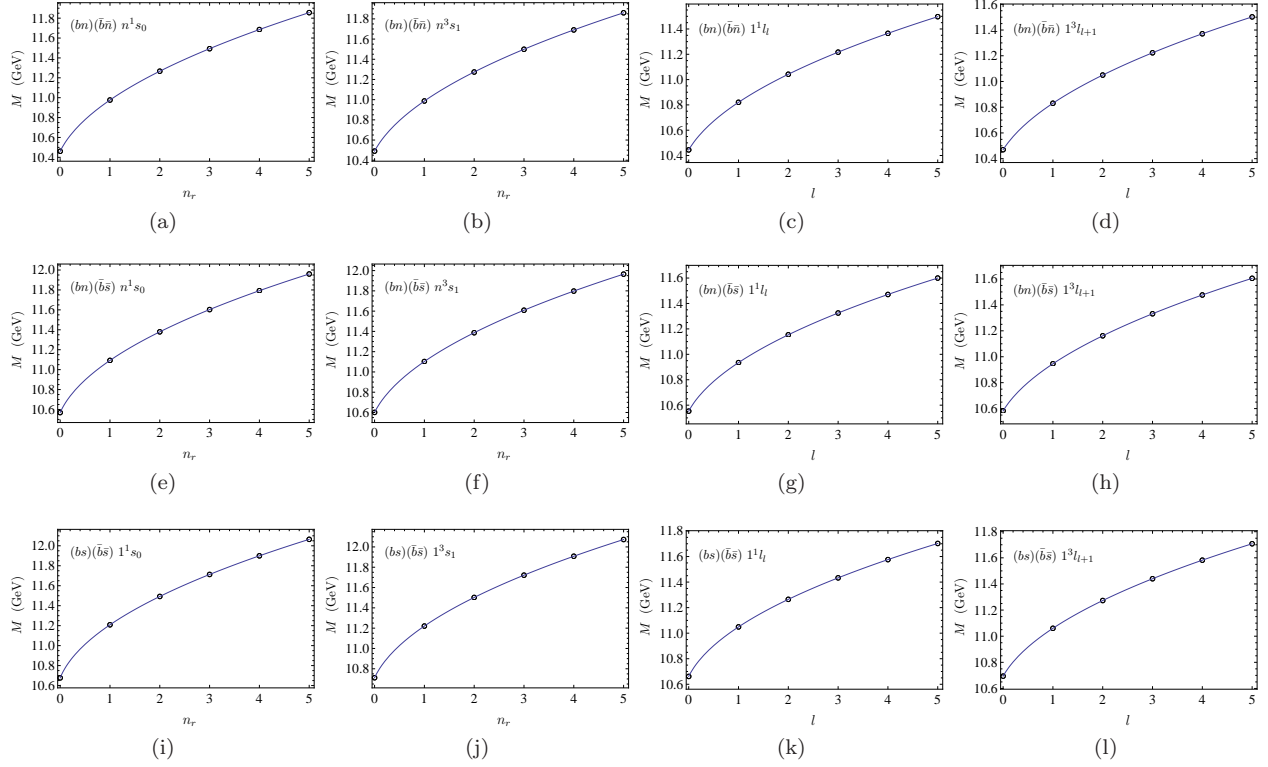


FIG. 3: The  $\rho$ -trajectories for the hidden bottom tetraquarks. Circles indicate the predicted data and the blue lines are the  $\rho$ -trajectories, see Eq. (2). Data are listed in Table IV.  $M$  is the bound state mass.  $n_r$  and  $l$  are the radial and orbital quantum numbers for the  $\rho$ -mode, respectively.  $1^1s_0$  and  $1^1l_l$  denote the spin singlet states.  $1^3s_1$  and  $1^3l_{l+1}$  represent the spin triplet states.

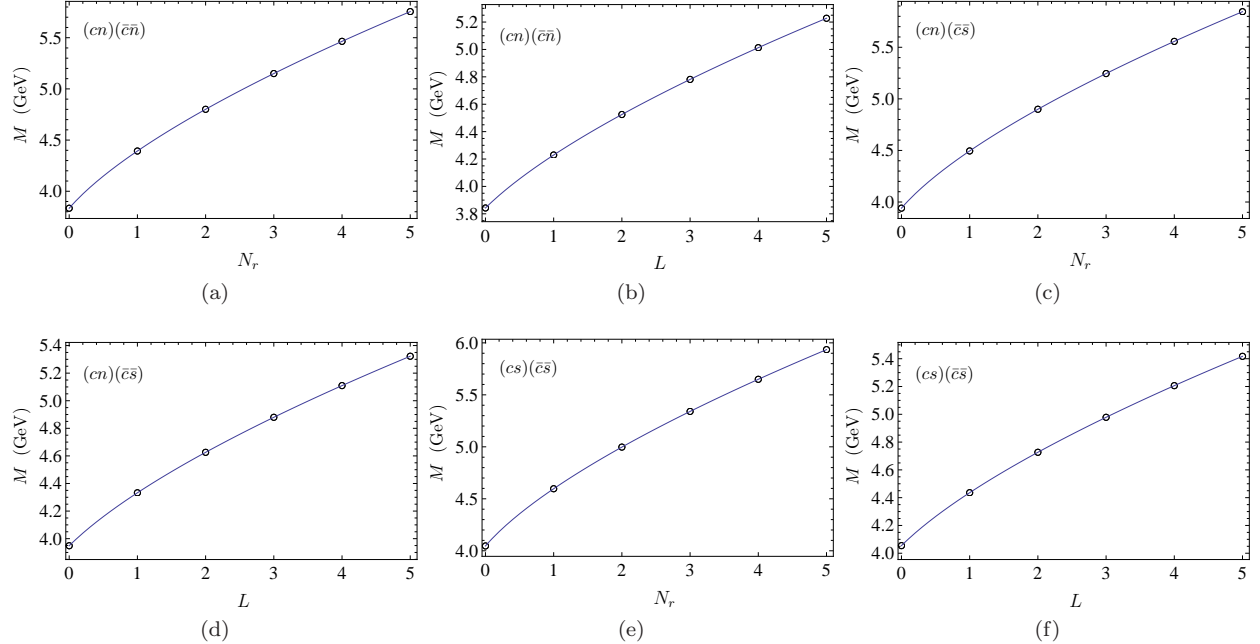


FIG. 4: Same as Fig. 2 except for the hidden charm tetraquarks and Table VI.

TABLE IV: The masses of the  $\rho$ -mode excited states of the hidden bottom tetraquarks (in GeV). The notation in Eq. (1) is rewritten as  $|n_1^{2s_1+1}l_{1j_1}, n_2^{2s_2+1}l_{2j_2}, N^{2j+1}L_J\rangle$ .  $(M', M'')$  is for  $(|n_1^{2s_1+1}l_{1j_1}, n_2^{2s_2+1}l_{2j_2}, N^{2j+1}L_J\rangle, |n_2^{2s_2+1}l_{2j_2}, n_1^{2s_1+1}l_{1j_1}, N^{2j+1}L_J\rangle)$ . For  $(bn)(\bar{b}\bar{n})$  and  $(bs)(\bar{b}\bar{s})$ ,  $M' = M''$ .  $n = u, d$ . Eqs. (2), (D2) and (D3) are used.

$ n_1^{2s_1+1}l_{1j_1}, n_2^{2s_2+1}l_{2j_2}, N^{2j+1}L_J\rangle$	$(bn)(\bar{b}\bar{n})$ $M' = M''$	$(bn)(\bar{b}\bar{s})$ $(M', M'')$	$(bs)(\bar{b}\bar{s})$ $M' = M''$
$ 1^1s_0, 1^1s_0, 1^1S_0\rangle$	10.46	(10.57, 10.57)	10.68
$ 2^1s_0, 1^1s_0, 1^1S_0\rangle$	10.98	(11.08, 11.10)	11.21
$ 3^1s_0, 1^1s_0, 1^1S_0\rangle$	11.27	(11.37, 11.38)	11.49
$ 4^1s_0, 1^1s_0, 1^1S_0\rangle$	11.49	(11.60, 11.61)	11.71
$ 5^1s_0, 1^1s_0, 1^1S_0\rangle$	11.69	(11.79, 11.79)	11.90
$ 1^3s_1, 1^1s_0, 1^3S_1\rangle$	10.49	(10.60, 10.60)	10.71
$ 2^3s_1, 1^1s_0, 1^3S_1\rangle$	10.99	(11.09, 11.11)	11.22
$ 3^3s_1, 1^1s_0, 1^3S_1\rangle$	11.27	(11.38, 11.39)	11.50
$ 4^3s_1, 1^1s_0, 1^3S_1\rangle$	11.50	(11.61, 11.61)	11.72
$ 5^3s_1, 1^1s_0, 1^3S_1\rangle$	11.69	(11.80, 11.80)	11.91
$ 1^1s_0, 1^1s_0, 1^1S_0\rangle$	10.44	(10.55, 10.55)	10.66
$ 1^1p_1, 1^1s_0, 1^3S_1\rangle$	10.82	(10.93, 10.94)	11.05
$ 1^1d_2, 1^1s_0, 1^5S_2\rangle$	11.04	(11.15, 11.16)	11.26
$ 1^1f_3, 1^1s_0, 1^7S_3\rangle$	11.22	(11.32, 11.33)	11.43
$ 1^1g_4, 1^1s_0, 1^9S_4\rangle$	11.37	(11.47, 11.47)	11.58
$ 1^1h_5, 1^1s_0, 1^{11}S_5\rangle$	11.50	(11.60, 11.59)	11.70
$ 1^3s_1, 1^1s_0, 1^3S_1\rangle$	10.47	(10.58, 10.59)	10.69
$ 1^3p_2, 1^1s_0, 1^5S_2\rangle$	10.83	(10.94, 10.95)	10.06
$ 1^3d_3, 1^1s_0, 1^7S_3\rangle$	11.05	(11.16, 11.17)	11.27
$ 1^3f_4, 1^1s_0, 1^9S_4\rangle$	11.22	(11.33, 11.33)	11.44
$ 1^3g_5, 1^1s_0, 1^{11}S_5\rangle$	11.37	(11.48, 11.47)	11.58
$ 1^3h_6, 1^1s_0, 1^{13}S_6\rangle$	11.50	(11.61, 11.60)	11.71

TABLE V: Comparison of theoretical predictions and experimental results (in GeV).  $C$  is defined only for  $q = q'$ .  $|n_1^{2s_1+1}l_{1j_1}, n_2^{2s_2+1}l_{2j_2}, N^{2j+1}L_J\rangle$  is defined in Eq. (4).

$J^{PC}$	Tetraquark	Name	State candidate $ n_1^{2s_1+1}l_{1j_1}, n_2^{2s_2+1}l_{2j_2}, N^{2j+1}L_J\rangle$	Our	PDG [49]	FGS [10]
$1^{+-}$	$(cn)(\bar{c}\bar{n})$	$T_{c\bar{c}1}(3900)^+$	$ 1^3s_1, 1^1s_0, 1^3S_1\rangle'$	3.95	3.8871	3.871
		$T_{c\bar{c}1}(4430)^+$	$ 1^3s_1, 1^3s_1, 1^3S_1\rangle'$			3.890
			$ 2^3s_1, 1^1s_0, 1^3S_1\rangle'$	4.44	4.478	
	$(cn)(\bar{c}\bar{s})$		$ 1^3s_1, 2^1s_0, 1^3S_1\rangle'$	4.51		
		$T_{c\bar{c}\bar{s}1}(4000)^+$	$ 1^3s_1, 1^1s_0, 2^3S_1\rangle'$	4.50		4.431
			$ 1^3s_1, 1^3s_1, 2^3S_1\rangle'$			4.461
$(bn)(\bar{b}\bar{n})$	$T_{b\bar{b}1}(10610)^+$		$ 1^3s_1, 1^1s_0, 1^3S_1\rangle'$	4.05	3.988	3.982
			$ 1^3s_1, 1^3s_1, 1^3S_1\rangle'$			4.004

The mass of the state  $|n_1^{2s_1+1}l_{1j_1}, n_2^{2s_2+1}l_{2j_2}, N^{2j+1}L_J\rangle$  for  $(cq)(\bar{c}\bar{q}')$  is equal to that of the state  $|n_2^{2s_2+1}l_{2j_2}, n_1^{2s_1+1}l_{1j_1}, N^{2j+1}L_J\rangle$  for  $(cq')(\bar{c}\bar{q})$ . For the  $\rho$ -mode excited states, the mass of the state  $|n_1^{2s_1+1}l_{1j_1}, n_2^{2s_2+1}l_{2j_2}, N^{2j+1}L_J\rangle$  with definite parity and charge parity (for  $q = q'$ )  $1/\sqrt{2}[(cq)(\bar{c}\bar{q}') \pm (cq')(\bar{c}\bar{q})]$  is equal to that of state

$$\begin{aligned} & |n_1^{2s_1+1}l_{1j_1}, n_2^{2s_2+1}l_{2j_2}, N^{2j+1}L_J\rangle' \\ &= \frac{1}{\sqrt{2}} \left( |n_1^{2s_1+1}l_{1j_1}, n_2^{2s_2+1}l_{2j_2}, N^{2j+1}L_J\rangle \right. \\ &\quad \left. \pm |n_2^{2s_2+1}l_{2j_2}, n_1^{2s_1+1}l_{1j_1}, N^{2j+1}L_J\rangle \right) \end{aligned}$$

for  $(cq)(\bar{c}\bar{q}')$  if  $n_1^{2s_1+1}l_{1j_1}$  is not identical to  $n_2^{2s_2+1}l_{2j_2}$ . The corresponding masses should be  $M = (M' + M'')/2$ , where  $M'$  and  $M''$  are listed in Table VIII. Therefore, the corresponding tetraquarks will be degenerate in mass. The  $\rho$ -trajectories are shown in Fig. 5.

In Ref. [10],  $T_{c\bar{c}1}(3900)^+$  and  $T_{c\bar{c}\bar{s}1}(4000)^+$  are regarded as  $|1^3s_1, 1^1s_0, 1^3S_1\rangle'$  and  $|1^3s_1, 1^3s_1, 1^3S_1\rangle'$  states, respectively. The masses of  $T_{c\bar{c}1}(3900)^+$  and  $T_{c\bar{c}\bar{s}1}(4000)^+$  coincide with the theoretical predictions for the  $1^+$  states,  $|1^3s_1, 1^1s_0, 1^3S_1\rangle'$  and  $|1^3s_1, 1^3s_1, 1^3S_1\rangle$ , see Table V. The observed  $T_{c\bar{c}1}(4430)^+$  has the same  $J^{PC}$  and quark content as  $T_{c\bar{c}1}(3900)^+$ . Its mass is  $4.478_{-18}^{+15}$  GeV [49]. In Ref. [21],  $T_{c\bar{c}1}(4430)^+$  is regarded as the

TABLE VI: The masses of the  $\lambda$ -mode excited states of the hidden charm tetraquarks (in GeV). The notation in Eq. (1) is rewritten as  $|n_1^{2s_1+1}l_{1j_1}, n_2^{2s_2+1}l_{2j_2}, N^{2j+1}L_J\rangle$ .  $n = u, d$ . Eqs. (2), (D2) and (D3) are used.

$ n_1^{2s_1+1}l_{1j_1}, n_2^{2s_2+1}l_{2j_2}, N^{2j+1}L_J\rangle$	$(cn)(\bar{c}\bar{n})$	$(cn)(\bar{c}\bar{s})$	$(cs)(\bar{c}\bar{s})$
$ 1^1s_0, 1^1s_0, 1^1S_0\rangle$	3.83	3.94	4.05
$ 1^1s_0, 1^1s_0, 2^1S_0\rangle$	4.39	4.50	4.60
$ 1^1s_0, 1^1s_0, 3^1S_0\rangle$	4.80	4.90	5.00
$ 1^1s_0, 1^1s_0, 4^1S_0\rangle$	5.15	5.25	5.34
$ 1^1s_0, 1^1s_0, 5^1S_0\rangle$	5.46	5.56	5.65
$ 1^1s_0, 1^1s_0, 1^1S_0\rangle$	3.84	3.95	4.05
$ 1^1s_0, 1^1s_0, 1^1P_1\rangle$	4.23	4.33	4.44
$ 1^1s_0, 1^1s_0, 1^1D_2\rangle$	4.52	4.63	4.73
$ 1^1s_0, 1^1s_0, 1^1F_3\rangle$	4.78	4.88	4.98
$ 1^1s_0, 1^1s_0, 1^1G_4\rangle$	5.01	5.11	5.21
$ 1^1s_0, 1^1s_0, 1^1H_5\rangle$	5.23	5.32	5.42

TABLE VII: Comparison of theoretical predictions for the masses of the hidden charm tetraquarks (in GeV).  $C$  is defined only for  $q = q'$ .

$J^{PC}$	$ n_1^{2s_1+1}l_{1j_1}, n_2^{2s_2+1}l_{2j_2}, N^{2j+1}L_J\rangle$	Tetraquark	Our	FGS [10]	FS [14]	TR [12]	HK [21]	GLM [18, 19]
$0^{++}$	$ 1^1s_0, 1^1s_0, 1^1S_0\rangle$	$(cn)(\bar{c}\bar{n})$	3.83	3.812			3.739	3.8419
		$(cn)(\bar{c}\bar{s})$	3.94	3.922	3.852	3.955		3.9518
		$(cs)(\bar{c}\bar{s})$	4.05	4.051		4.045	3.946	
	$ 1^1s_0, 1^1s_0, 2^1S_0\rangle$	$(cn)(\bar{c}\bar{n})$	4.39	4.375			4.357	
		$(cn)(\bar{c}\bar{s})$	4.50	4.481	4.383	4.500		
		$(cs)(\bar{c}\bar{s})$	4.60	4.604		4.620	4.558	
	$ 1^1s_0, 1^1s_0, 1^1P_1\rangle$	$(cn)(\bar{c}\bar{n})$	4.23	4.244			4.231	4.2244
		$(cn)(\bar{c}\bar{s})$	4.33	4.350	4.234	4.413		
		$(cs)(\bar{c}\bar{s})$	4.44	4.466		4.556	4.464	

TABLE VIII: The masses of the  $\rho$ -mode excited states of the hidden charm tetraquarks (in GeV). The notation in Eq. (1) is rewritten as  $|n_1^{2s_1+1}l_{1j_1}, n_2^{2s_2+1}l_{2j_2}, N^{2j+1}L_J\rangle$ .  $(M', M'')$  is for  $(|n_1^{2s_1+1}l_{1j_1}, n_2^{2s_2+1}l_{2j_2}, N^{2j+1}L_J\rangle, |n_2^{2s_2+1}l_{2j_2}, n_1^{2s_1+1}l_{1j_1}, N^{2j+1}L_J\rangle)$ . For  $(cn)(\bar{c}\bar{n})$  and  $(cs)(\bar{c}\bar{s})$ ,  $M' = M''$ .  $n = u, d$ . Equations (2), (D2), and (D3) are used.

$ n_1^{2s_1+1}l_{1j_1}, n_2^{2s_2+1}l_{2j_2}, N^{2j+1}L_J\rangle$	$(cn)(\bar{c}\bar{n})$ $M' = M''$	$(cn)(\bar{c}\bar{s})$ $(M', M'')$	$(cs)(\bar{c}\bar{s})$ $M' = M''$
$ 1^1s_0, 1^1s_0, 1^1S_0\rangle$	3.83	(3.94, 3.94)	4.05
$ 2^1s_0, 1^1s_0, 1^1S_0\rangle$	4.40	(4.50, 4.56)	4.67
$ 3^1s_0, 1^1s_0, 1^1S_0\rangle$	4.70	(4.80, 4.87)	4.97
$ 4^1s_0, 1^1s_0, 1^1S_0\rangle$	4.93	(5.03, 5.11)	5.21
$ 5^1s_0, 1^1s_0, 1^1S_0\rangle$	5.12	(5.23, 5.31)	5.41
$ 1^3s_1, 1^1s_0, 1^3S_1\rangle$	3.95	(4.05, 4.04)	4.15
$ 2^3s_1, 1^1s_0, 1^3S_1\rangle$	4.44	(4.54, 4.59)	4.69
$ 3^3s_1, 1^1s_0, 1^3S_1\rangle$	4.72	(4.83, 4.89)	4.99
$ 4^3s_1, 1^1s_0, 1^3S_1\rangle$	4.95	(5.05, 5.12)	5.23
$ 5^3s_1, 1^1s_0, 1^3S_1\rangle$	5.14	(5.25, 5.32)	5.42
$ 1^1s_0, 1^1s_0, 1^1S_0\rangle$	3.83	(3.94, 3.95)	4.06
$ 1^1p_1, 1^1s_0, 1^3S_1\rangle$	4.28	(4.38, 4.42)	4.52
$ 1^1d_2, 1^1s_0, 1^5S_2\rangle$	4.52	(4.63, 4.66)	4.76
$ 1^1f_3, 1^1s_0, 1^7S_3\rangle$	4.71	(4.82, 4.85)	4.95
$ 1^1g_4, 1^1s_0, 1^9S_4\rangle$	4.87	(4.98, 5.00)	5.11
$ 1^1h_5, 1^1s_0, 1^{11}S_5\rangle$	5.01	(5.12, 5.14)	5.25
$ 1^3s_1, 1^1s_0, 1^3S_1\rangle$	3.91	(4.02, 4.03)	4.13
$ 1^3p_2, 1^1s_0, 1^5S_2\rangle$	4.30	(4.41, 4.44)	4.55
$ 1^3d_3, 1^1s_0, 1^7S_3\rangle$	4.54	(4.65, 4.68)	4.78
$ 1^3f_4, 1^1s_0, 1^9S_4\rangle$	4.73	(4.83, 4.86)	4.96
$ 1^3g_5, 1^1s_0, 1^{11}S_5\rangle$	4.89	(4.99, 5.02)	5.12
$ 1^3h_6, 1^1s_0, 1^{13}S_6\rangle$	5.03	(5.13, 5.16)	5.26

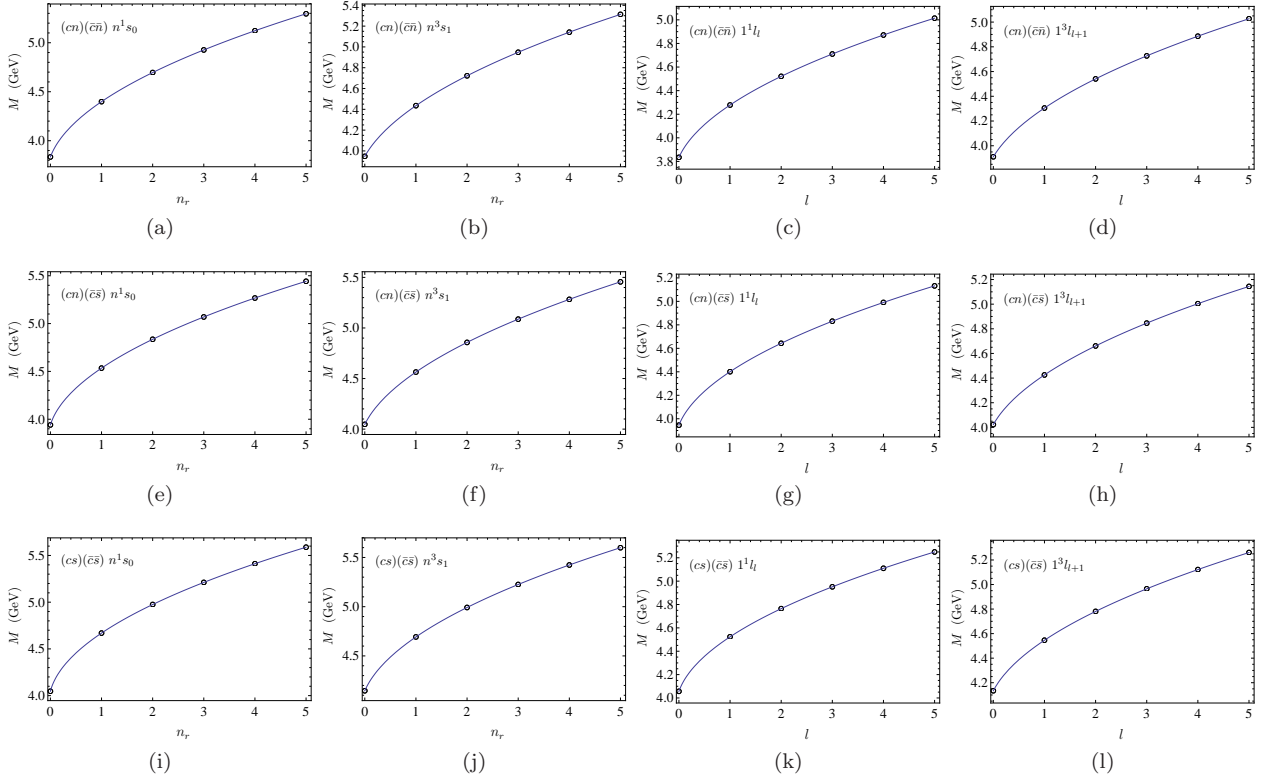


FIG. 5: Same as Fig. 3 except for the hidden charm tetraquarks and Table VIII.

first radially  $\lambda$ -excited state  $|1^3s_1, 1^3s_1, 2^3S_1\rangle$  of  $(cn)(\bar{c}\bar{n})$ . In Ref. [10],  $T_{c\bar{c}1}(4430)^+$  is taken as  $|1^3s_1, 1^3s_1, 2^3S_1\rangle$  state or  $|1^3s_1, 1^1s_0, 2^3S_1\rangle'$  state. The mass of  $T_{c\bar{c}1}(4430)^+$  also approximates the mass of the  $|2^3s_1, 1^1s_0, 1^3S_1\rangle'$  state and the  $|1^3s_1, 2^1s_0, 1^3S_1\rangle'$  state, see Table VIII. The states  $|2^3s_1, 1^1s_0, 1^3S_1\rangle'$  and  $|1^3s_1, 2^1s_0, 1^3S_1\rangle'$  are the  $\rho$ -excited states. We conclude that  $T_{c\bar{c}1}(4430)^+$  is possibly the first radial  $\lambda$ -excitation or the first radial  $\rho$ -excitation.

## F. Discussions

By employing the Regge trajectory formulas in (2), the masses for the more highly excited states can be calculated easily. We argue that the calculation of the masses of highly excited state is instructive although the highly excited states will be unstable. This is because various models or approaches to calculate the masses of tetraquarks often use different parameter values. These models, despite using different parameter values, often give agreeable predictions for the ground state and the lower excited states. The theoretical predictions for the highly excited states are expected to show differences, which will be instructive.

The Regge trajectories take different form and behave differently in various energy regions [28, 32]. The hidden charm tetraquark case is similar to the hidden bottom tetraquark case. Both the diquark ( $Qq$ ) and

antidiquark ( $\bar{Q}\bar{q}'$ ) are the heavy-light systems; therefore, the  $\rho$ -trajectories of the hidden bottom and charm tetraquarks behave as  $M \sim x_\rho^{1/2}$ , see Eq. (2). For the  $\lambda$ -mode, the tetraquark ( $Qq(\bar{Q}\bar{q}')$ ) is the heavy-heavy system; hence, the  $\lambda$ -trajectories of the hidden bottom and charm tetraquarks behave as  $M \sim x_\lambda^{2/3}$ .

According to Eq. (2), there are three series of Regge trajectories: two series of  $\rho$ -trajectories and one series of  $\lambda$ -trajectories. Correspondingly, there are three series of masses. When  $q = q'$ , there is degeneracy in the  $\rho$ -trajectories, corresponding to the degeneracy in masses of the  $\rho$ -excited states.

For the hidden bottom and charm tetraquarks, both the  $\lambda$ -trajectories and the  $\rho$ -trajectories are concave downward in the  $(M^2, x)$  planes if the confining potential is linear. In the subsection C4, we show that for all tetraquarks, not only the  $\lambda$ -trajectories but also the  $\rho$ -trajectories are concave downward in the  $(M^2, x)$  planes when the masses of the light constituents are considered and the confining potential is linear.

## III. CONCLUSIONS

In this work, we obtain the Regge trajectory formulas for the hidden bottom and charm tetraquarks ( $Qq(\bar{Q}\bar{q}')$ ) by using the Regge trajectory formula for the heavy-heavy systems and the newly proposed Regge tra-

trajectory relation for the heavy-light diquarks. We apply the obtained Regge trajectory formulas to investigate the tetraquarks with hidden bottom and charm. The masses of the  $\lambda$ -mode excited and  $\rho$ -mode excited tetraquarks are estimated. The calculated results are in agreement with other theoretical predictions. Both the  $\lambda$ -trajectories and  $\rho$ -trajectories are discussed.

For the hidden bottom and charm tetraquarks, there are three series of the Regge trajectories: two series of  $\rho$ -trajectories and one series of  $\lambda$ -trajectories. They exhibit different behaviors. The  $\rho$ -trajectories behave as  $M \sim x_\rho^{1/2}$  because the  $\rho$ -mode excitations are in the heavy-light diquark ( $Qq$ ) and antidiquark ( $\bar{Q}\bar{q}'$ ). In contrast, the  $\lambda$ -trajectories behave as  $M \sim x_\lambda^{2/3}$  because the  $\lambda$ -mode excitations occur between the diquark and the antidiquark, with the diquark ( $Qq$ ) and antidiquark ( $\bar{Q}\bar{q}'$ ) forming a heavy-heavy system ( $Qq)(\bar{Q}\bar{q}'$ ).

Moreover, the behaviors of the Regge trajectories for various tetraquarks are investigated based on the spinless Salpeter equation. It is shown that both the  $\lambda$ -trajectories and the  $\rho$ -trajectories for all tetraquarks are concave downward in the  $(M^2, x)$  plane when the masses of the light constituents are considered and the confining potential is linear.

### Acknowledgments

We are very grateful to the anonymous referees for the valuable comments and suggestions.

### Appendix A: States of diquarks

TABLE IX: The completely antisymmetric states for the diquarks in  $3_c$  [47].  $j$  is the spin of the diquark ( $qq'$ ),  $s$  denotes the total spin of two quarks,  $l$  represents the orbital angular momentum.  $n = n_r + 1$ ,  $n_r$  is the radial quantum number,  $n_r = 0, 1, 2, \dots$ .

Spin of diquark ( $j$ )	Parity ( $j^P$ )	Wave state ( $n^{2s+1}l_j$ )	Configuration
$j=0$	$0^+$	$n^1 s_0$	$[qq']_{n^1 s_0}^{3_c}$
	$0^-$	$n^3 p_0$	$[qq']_{n^3 p_0}^{3_c}$
$j=1$	$1^+$	$n^3 s_1, n^3 d_1$	$\{qq'\}_{n^3 s_1}^{3_c}, \{qq'\}_{n^3 d_1}^{3_c}$
	$1^-$	$n^1 p_1, n^3 p_1$	$\{qq'\}_{n^1 p_1}^{3_c}, [qq']_{n^3 p_1}^{3_c}$
$j=2$	$2^+$	$n^1 d_2, n^3 d_2$	$[qq']_{n^1 d_2}^{3_c}, \{qq'\}_{n^3 d_2}^{3_c}$
	$2^-$	$n^3 p_2, n^3 f_2$	$[qq']_{n^3 p_2}^{3_c}, [qq']_{n^3 f_2}^{3_c}$
...	...	...	...

In this section, we list the completely antisymmetric states for the diquarks in  $3_c$  [47], see Table IX.

### Appendix B: States of tetraquarks

The states of tetraquark in the diquark picture are listed in Table X.

### Appendix C: Regge trajectory behaviors for various tetraquarks

In this section, the Regge trajectory behaviors for various tetraquarks are investigated.

#### 1. Spinless Salpeter equation

The spinless Salpeter equation [50–56] reads as

$$M\Psi_{d,t}(\mathbf{r}) = (\omega_1 + \omega_2)\Psi_{d,t}(\mathbf{r}) + V_{d,t}\Psi_{d,t}(\mathbf{r}), \quad (C1)$$

where  $M$  is the bound state mass (diquark or tetraquark).  $\Psi_{d,t}(\mathbf{r})$  are the diquark wave function and the tetraquark wave function, respectively.  $V_{d,t}$  denotes the diquark potential and the tetraquark potential, respectively (see Eq. (C3)).  $\omega_1$  is the relativistic energy of constituent 1 (quark or diquark), and  $\omega_2$  is of constituent 2 (quark or antidiquark),

$$\omega_i = \sqrt{m_i^2 + \mathbf{p}^2} = \sqrt{m_i^2 - \Delta} \quad (i = 1, 2). \quad (C2)$$

$m_1$  and  $m_2$  are the effective masses of constituent 1 and 2, respectively.

When using diquark in multiquark systems, the interactions between quark and quark, diquark and quark, diquark and diquark are needed. In Refs. [10], these interactions are constructed with the help of the off-mass-shell scattering amplitude, which is projected onto the positive energy states. The interactions also can be established by expanding the interactions of the quark-antiquark system to the quark-quark system, and then to the diquark-antidiquark systems or the diquark-quark systems [13]. Furthermore, the effect of the finite size of diquark is treated differently. In Refs. [10], the size of diquark is taken into account through corresponding form factors. At times, diquark is taken as being pointlike [13, 51], and we use this approximation in the present work.

Following Refs. [50, 51, 57, 58], we employ the potential

$$V_{d,t} = -\frac{3}{4} [V_c + \sigma r + C] (\mathbf{F}_i \cdot \mathbf{F}_j)_{d,t}, \quad (C3)$$

where  $V_c \propto 1/r$  is a color Coulomb potential or a Coulomb-like potential due to one-gluon-exchange.  $\sigma$  is the string tension.  $C$  is a fundamental parameter [59, 60]. The part in the bracket is the Cornell potential [58].  $\mathbf{F}_i \cdot \mathbf{F}_j$  is the color-Casimir,

$$\langle (\mathbf{F}_i \cdot \mathbf{F}_j)_d \rangle = -\frac{2}{3}, \quad \langle (\mathbf{F}_i \cdot \mathbf{F}_j)_t \rangle = -\frac{4}{3}. \quad (C4)$$

TABLE X: The states of tetraquark in the diquark picture. The diquark notation is in IX. Here,  $q$  and  $q'$  represent both the light quarks and the heavy quarks. The superscript  $1_c$  is omitted.

$J^P$	$(l_1, l_2, L)$	Configuration
$0^+$	$(0, 0, 0)$	$\left( [qq']_{n_1^1 s_0}^{3_c} [\bar{q}\bar{q}']_{n_2^1 s_0}^{3_c} \right)_{N^1 S_0}, \left( \{qq'\}_{n_1^3 s_1}^{3_c} \{ \bar{q}\bar{q}' \}_{n_2^3 s_1}^{3_c} \right)_{N^1 S_0},$
	$(1, 1, 0)$	$\left( [qq']_{n_1^3 p_0}^{3_c} [\bar{q}\bar{q}']_{n_2^3 p_0}^{3_c} \right)_{N^1 S_0}, \left( \{qq'\}_{n_1^1 p_1}^{3_c} \{ \bar{q}\bar{q}' \}_{n_2^1 p_1}^{3_c} \right)_{N^1 S_0}, \left( [qq']_{n_1^3 p_1}^{3_c} [\bar{q}\bar{q}']_{n_2^3 p_1}^{3_c} \right)_{N^1 S_0}, \left( [qq']_{n_1^3 p_2}^{3_c} [\bar{q}\bar{q}']_{n_2^3 p_2}^{3_c} \right)_{N^1 S_0}, \left( \{qq'\}_{n_1^1 p_1}^{3_c} \{ \bar{q}\bar{q}' \}_{n_2^3 p_1}^{3_c} \right)_{N^1 S_0}, \left( \{qq'\}_{n_1^3 p_1}^{3_c} \{ \bar{q}\bar{q}' \}_{n_2^1 p_1}^{3_c} \right)_{N^1 S_0}$
	$(0, 1, 1)$	$\left( [qq']_{n_1^1 s_0}^{3_c} \{ \bar{q}\bar{q}' \}_{n_2^1 p_1}^{3_c} \right)_{N^3 P_0}, \left( [qq']_{n_1^3 s_0}^{3_c} [\bar{q}\bar{q}']_{n_2^3 p_1}^{3_c} \right)_{N^3 P_0}, \left( \{qq'\}_{n_1^3 s_1}^{3_c} [\bar{q}\bar{q}']_{n_2^3 p_0}^{3_c} \right)_{N^3 P_0},$
		$\left( \{qq'\}_{n_1^1 s_1}^{3_c} \{ \bar{q}\bar{q}' \}_{n_2^1 p_1}^{3_c} \right)_{N^3 P_0}, \left( \{qq'\}_{n_1^3 s_1}^{3_c} [\bar{q}\bar{q}']_{n_2^3 p_1}^{3_c} \right)_{N^3 P_0}, \left( \{qq'\}_{n_1^3 s_1}^{3_c} [\bar{q}\bar{q}']_{n_2^3 p_2}^{3_c} \right)_{N^3 P_0}$
	$(1, 0, 1)$	$\left( \{qq'\}_{n_1^1 p_1}^{3_c} [\bar{q}\bar{q}']_{n_2^1 s_0}^{3_c} \right)_{N^3 P_0}, \left( [qq']_{n_1^3 p_1}^{3_c} [\bar{q}\bar{q}']_{n_2^3 s_0}^{3_c} \right)_{N^3 P_0}, \left( [qq']_{n_1^3 p_0}^{3_c} \{ \bar{q}\bar{q}' \}_{n_2^3 s_1}^{3_c} \right)_{N^3 P_0},$
		$\left( \{qq'\}_{n_1^1 p_1}^{3_c} \{ \bar{q}\bar{q}' \}_{n_2^3 s_1}^{3_c} \right)_{N^3 P_0}, \left( [qq']_{n_1^3 p_1}^{3_c} \{ \bar{q}\bar{q}' \}_{n_2^1 s_1}^{3_c} \right)_{N^3 P_0}, \left( [qq']_{n_1^3 p_2}^{3_c} \{ \bar{q}\bar{q}' \}_{n_2^3 s_1}^{3_c} \right)_{N^3 P_0}$
	...	...
$0^-$	$(0, 0, 1)$	$\left( [qq']_{n_1^1 s_0}^{3_c} \{ \bar{q}\bar{q}' \}_{n_2^3 s_1}^{3_c} \right)_{N^3 P_0}, \left( \{qq'\}_{n_1^3 s_1}^{3_c} [\bar{q}\bar{q}']_{n_2^1 s_0}^{3_c} \right)_{N^3 P_0}, \left( \{qq'\}_{n_1^3 s_1}^{3_c} \{ \bar{q}\bar{q}' \}_{n_2^3 s_1}^{3_c} \right)_{N^3 P_0},$
	$(1, 0, 0)$	$\left( [qq']_{n_1^3 p_0}^{3_c} [\bar{q}\bar{q}']_{n_2^1 s_0}^{3_c} \right)_{N^1 S_0}, \left( \{qq'\}_{n_1^1 p_1}^{3_c} \{ \bar{q}\bar{q}' \}_{n_2^3 s_0}^{3_c} \right)_{N^1 S_0}, \left( [qq']_{n_1^3 p_1}^{3_c} \{ \bar{q}\bar{q}' \}_{n_2^3 s_1}^{3_c} \right)_{N^1 S_0},$
	$(0, 1, 0)$	$\left( [qq']_{n_1^1 s_0}^{3_c} [\bar{q}\bar{q}']_{n_2^3 p_0}^{3_c} \right)_{N^1 S_0}, \left( \{qq'\}_{n_1^3 s_1}^{3_c} \{ \bar{q}\bar{q}' \}_{n_2^1 p_1}^{3_c} \right)_{N^1 S_0}, \left( \{qq'\}_{n_1^3 s_1}^{3_c} [\bar{q}\bar{q}']_{n_2^3 p_1}^{3_c} \right)_{N^1 S_0}$
	...	...
$1^+$	$(0, 0, 0)$	$\left( [qq']_{n_1^1 s_0}^{3_c} \{ \bar{q}\bar{q}' \}_{n_2^3 s_1}^{3_c} \right)_{N^3 S_1}, \left( \{qq'\}_{n_1^3 s_1}^{3_c} [\bar{q}\bar{q}']_{n_2^1 s_0}^{3_c} \right)_{N^3 S_1}, \left( \{qq'\}_{n_1^3 s_1}^{3_c} \{ \bar{q}\bar{q}' \}_{n_2^3 s_1}^{3_c} \right)_{N^3 S_1},$
	$(1, 1, 0)$	$\left( [qq']_{n_1^3 p_0}^{3_c} \{ \bar{q}\bar{q}' \}_{n_2^1 p_1}^{3_c} \right)_{N^3 S_1}, \left( [qq']_{n_1^3 p_0}^{3_c} [\bar{q}\bar{q}']_{n_2^3 p_1}^{3_c} \right)_{N^3 S_1},$
		$\left( \{qq'\}_{n_1^1 p_1}^{3_c} [\bar{q}\bar{q}']_{n_2^3 p_0}^{3_c} \right)_{N^3 S_1}, \left( \{qq'\}_{n_1^1 p_1}^{3_c} \{ \bar{q}\bar{q}' \}_{n_2^1 p_1}^{3_c} \right)_{N^3 S_1}, \left( \{qq'\}_{n_1^1 p_1}^{3_c} [\bar{q}\bar{q}']_{n_2^3 p_1}^{3_c} \right)_{N^3 S_1}, \left( \{qq'\}_{n_1^1 p_1}^{3_c} [\bar{q}\bar{q}']_{n_2^3 p_2}^{3_c} \right)_{N^3 S_1},$
		$\left( [qq']_{n_1^3 p_1}^{3_c} [\bar{q}\bar{q}']_{n_2^3 p_0}^{3_c} \right)_{N^3 S_1}, \left( [qq']_{n_1^3 p_1}^{3_c} \{ \bar{q}\bar{q}' \}_{n_2^3 p_1}^{3_c} \right)_{N^3 S_1}, \left( [qq']_{n_1^3 p_1}^{3_c} [\bar{q}\bar{q}']_{n_2^3 p_2}^{3_c} \right)_{N^3 S_1}, \left( [qq']_{n_1^3 p_2}^{3_c} \{ \bar{q}\bar{q}' \}_{n_2^3 p_1}^{3_c} \right)_{N^3 S_1}, \left( [qq']_{n_1^3 p_2}^{3_c} [\bar{q}\bar{q}']_{n_2^3 p_2}^{3_c} \right)_{N^3 S_1},$
	$(0, 1, 1)$	$\left( [qq']_{n_1^1 s_0}^{3_c} \{ \bar{q}\bar{q}' \}_{n_2^1 p_1}^{3_c} \right)_{N^3 P_1}, \left( [qq']_{n_1^3 s_0}^{3_c} [\bar{q}\bar{q}']_{n_2^3 p_1}^{3_c} \right)_{N^3 P_1}, \left( \{qq'\}_{n_1^3 s_1}^{3_c} \{ \bar{q}\bar{q}' \}_{n_2^3 p_0}^{3_c} \right)_{N^3 P_1},$
		$\left( \{qq'\}_{n_1^3 s_1}^{3_c} \{ \bar{q}\bar{q}' \}_{n_2^1 p_1}^{3_c} \right)_{N^3 P_1}, \left( \{qq'\}_{n_1^3 s_1}^{3_c} [\bar{q}\bar{q}']_{n_2^3 p_1}^{3_c} \right)_{N^3 P_1}, \left( \{qq'\}_{n_1^3 s_1}^{3_c} [\bar{q}\bar{q}']_{n_2^3 p_2}^{3_c} \right)_{N^3 P_1},$
		$\left( \{qq'\}_{n_1^3 s_1}^{3_c} \{ \bar{q}\bar{q}' \}_{n_2^1 p_1}^{3_c} \right)_{N^5 P_1}, \left( \{qq'\}_{n_1^3 s_1}^{3_c} [\bar{q}\bar{q}']_{n_2^3 p_1}^{3_c} \right)_{N^5 P_1}, \left( \{qq'\}_{n_1^3 s_1}^{3_c} [\bar{q}\bar{q}']_{n_2^3 p_2}^{3_c} \right)_{N^5 P_1}$
	$(1, 0, 1)$	$\left( [qq']_{n_1^1 p_1}^{3_c} [\bar{q}\bar{q}']_{n_2^1 s_0}^{3_c} \right)_{N^3 P_1}, \left( [qq']_{n_1^3 p_1}^{3_c} [\bar{q}\bar{q}']_{n_2^3 s_0}^{3_c} \right)_{N^3 P_1}, \left( [qq']_{n_1^3 p_0}^{3_c} \{ \bar{q}\bar{q}' \}_{n_2^3 s_1}^{3_c} \right)_{N^3 P_1},$
		$\left( [qq']_{n_1^1 p_1}^{3_c} \{ \bar{q}\bar{q}' \}_{n_2^3 s_1}^{3_c} \right)_{N^3 P_1}, \left( [qq']_{n_1^3 p_1}^{3_c} [\bar{q}\bar{q}']_{n_2^1 s_1}^{3_c} \right)_{N^3 P_1}, \left( [qq']_{n_1^3 p_2}^{3_c} \{ \bar{q}\bar{q}' \}_{n_2^3 s_1}^{3_c} \right)_{N^3 P_1},$
		$\left( [qq']_{n_1^1 p_1}^{3_c} \{ \bar{q}\bar{q}' \}_{n_2^3 s_1}^{3_c} \right)_{N^5 P_1}, \left( [qq']_{n_1^3 p_1}^{3_c} [\bar{q}\bar{q}']_{n_2^3 s_1}^{3_c} \right)_{N^5 P_1}, \left( [qq']_{n_1^3 p_2}^{3_c} \{ \bar{q}\bar{q}' \}_{n_2^3 s_1}^{3_c} \right)_{N^5 P_1}$
	...	...
$1^-$	$(0, 0, 1)$	$\left( [qq']_{n_1^1 s_0}^{3_c} \{ \bar{q}\bar{q}' \}_{n_2^3 s_1}^{3_c} \right)_{N^3 P_1}, \left( \{qq'\}_{n_1^3 s_1}^{3_c} [\bar{q}\bar{q}']_{n_2^1 s_0}^{3_c} \right)_{N^3 P_1}, \left( \{qq'\}_{n_1^3 s_1}^{3_c} \{ \bar{q}\bar{q}' \}_{n_2^3 s_1}^{3_c} \right)_{N^3 P_1},$
		$\left( [qq']_{n_1^1 s_0}^{3_c} [\bar{q}\bar{q}']_{n_2^1 s_0}^{3_c} \right)_{N^1 P_1}, \left( \{qq'\}_{n_1^3 s_1}^{3_c} \{ \bar{q}\bar{q}' \}_{n_2^3 s_1}^{3_c} \right)_{N^1 P_1}, \left( \{qq'\}_{n_1^3 s_1}^{3_c} \{ \bar{q}\bar{q}' \}_{n_2^3 s_1}^{3_c} \right)_{N^5 P_1},$
		$\left( [qq']_{n_1^3 p_0}^{3_c} [\bar{q}\bar{q}']_{n_2^3 s_1}^{3_c} \right)_{N^3 S_1}, \left( \{qq'\}_{n_1^1 p_1}^{3_c} \{ \bar{q}\bar{q}' \}_{n_2^3 s_1}^{3_c} \right)_{N^3 S_1}, \left( \{qq'\}_{n_1^1 p_1}^{3_c} [\bar{q}\bar{q}']_{n_2^1 s_0}^{3_c} \right)_{N^3 S_1},$
		$\left( [qq']_{n_1^3 p_1}^{3_c} [\bar{q}\bar{q}']_{n_2^3 s_1}^{3_c} \right)_{N^3 S_1}, \left( [qq']_{n_1^3 p_1}^{3_c} [\bar{q}\bar{q}']_{n_2^1 s_0}^{3_c} \right)_{N^3 S_1}, \left( [qq']_{n_1^3 p_2}^{3_c} \{ \bar{q}\bar{q}' \}_{n_2^3 s_1}^{3_c} \right)_{N^3 S_1}$
	$(0, 1, 0)$	$\left( \{qq'\}_{n_1^3 s_1}^{3_c} [\bar{q}\bar{q}']_{n_2^1 s_0}^{3_c} \right)_{N^3 S_1}, \left( \{qq'\}_{n_1^3 s_1}^{3_c} \{ \bar{q}\bar{q}' \}_{n_2^1 p_1}^{3_c} \right)_{N^3 S_1}, \left( \{qq'\}_{n_1^3 s_1}^{3_c} \{ \bar{q}\bar{q}' \}_{n_2^1 p_1}^{3_c} \right)_{N^3 S_1},$
		$\left( \{qq'\}_{n_1^3 s_1}^{3_c} [\bar{q}\bar{q}']_{n_2^1 s_0}^{3_c} \right)_{N^5 P_1}, \left( \{qq'\}_{n_1^3 s_1}^{3_c} [\bar{q}\bar{q}']_{n_2^1 p_1}^{3_c} \right)_{N^5 P_1}, \left( \{qq'\}_{n_1^3 s_1}^{3_c} [\bar{q}\bar{q}']_{n_2^1 p_1}^{3_c} \right)_{N^5 P_1}$
	...	...

## 2. Regge trajectory relations for various systems

where

For the heavy-heavy systems,  $m_1, m_2 \gg |\mathbf{p}|$ , Eq. (C1) reduces to

$$M\Psi_{d,t}(\mathbf{r}) = \left[ (m_1 + m_2) + \frac{\mathbf{p}^2}{2\mu} \right] \Psi_{d,t}(\mathbf{r}) + V_{d,t} \Psi_{d,t}(\mathbf{r}), \quad (\text{C5})$$

By employing the Bohr-Sommerfeld quantization approach [61] and using Eqs. (C3) and (C5), we obtain

the parametrized relation [28, 32]

$$M = m_R + \beta_x(x + c_{0x})^{2/3} \quad (x = l, n_r, L, N_r), \quad (\text{C7})$$

with

$$\beta_x = c_{fx}c_xc_c, \quad m_R = m_1 + m_2 + C', \quad (\text{C8})$$

where

$$C' = \begin{cases} C/2, & \text{diquarks,} \\ C, & \text{tetraquarks.} \end{cases} \quad (\text{C9})$$

$$\sigma' = \begin{cases} \sigma/2, & \text{diquarks,} \\ \sigma, & \text{tetraquarks.} \end{cases} \quad (\text{C10})$$

$c_x$  and  $c_c$  are

$$c_c = \left( \frac{\sigma'^2}{\mu} \right)^{1/3}, \quad c_{l,L} = \frac{3}{2}, \quad c_{n_r,N_r} = \frac{(3\pi)^{2/3}}{2}. \quad (\text{C11})$$

$c_{fx}$  are equal theoretically to one and are fitted in practice. In Eq. (C7),  $m_1$ ,  $m_2$ ,  $c_x$  and  $\sigma$  are universal for the heavy-heavy systems.  $c_{0x}$  vary with different Regge trajectories.

For the heavy-light systems ( $m_1 \rightarrow \infty$  and  $m_2 \rightarrow 0$ ), Eq. (C1) simplifies to

$$M\Psi_{d,t}(\mathbf{r}) = [m_1 + |\mathbf{p}| + V_{d,t}] \Psi_{d,t}(\mathbf{r}). \quad (\text{C12})$$

By employing the Bohr-Sommerfeld quantization approach [61] and using Eq. (C12), the parameterized formula can be written as [28, 32]

$$M = m_R + \beta_x \sqrt{x + c_{0x}} \quad (x = l, n_r, L, N_r). \quad (\text{C13})$$

$\beta_x$  is in Eq. (C8), and with

$$c_c = \sqrt{\sigma'}, \quad c_{l,L} = 2, \quad c_{n_r,N_r} = \sqrt{2\pi}. \quad (\text{C14})$$

For the heavy-light systems, the common choice of  $m_R$  is [32, 42, 62–66]

$$m_R = m_1. \quad (\text{C15})$$

The usual Regge trajectory, Eq. (C13) with (C15), is obtained in the limit  $m_1 \rightarrow \infty$  and  $m_2 \rightarrow 0$ . There are different ways of including the light constituent's mass [28, 29, 42–46, 64, 67, 68]. Two modified formulas are proposed in Ref. [29], which can universally describe both the heavy-light mesons and the heavy-light diquarks. One is Eq. (C13) with  $m_R$  in (C8), where  $m_2$  is the light constituent's mass. Another reads

$$M = m_R + \sqrt{\beta_x^2(x + c_{0x}) + \kappa_x m_2^{3/2}(x + c_{0x})^{1/4}} \quad (\text{C16})$$

if  $m_2 \ll M$ , where

$$m_R = m_1 + C', \quad \kappa_x = \frac{4}{3}\sqrt{\pi\beta_x}, \quad (\text{C17})$$

where  $\beta_x$  is in (C8). Equation (C13) with (C8) is an extension of [67]

$$M = m_1 + m_2 + \sqrt{a(n_r + al + b)} \quad (\text{C18})$$

and the formula [28]

$$(M - m_1 - m_2 - C)^2 = \alpha_x(x + c_0)^\gamma \quad (\text{C19})$$

while (C16) with (C17) is based on the results in [42, 44]. As  $m_2 = 0$ , these two modified formulas, Eq. (C13) with (C8) and Eq. (C16) with (C17), become identical. As  $m_2 = 0$  and  $C$  is neglected, these two modified formulas reduce to the usual Regge trajectory formula for the heavy-light systems, i.e., (C13) with (C15). Although they give different behavior of  $m_2$ , Eq. (C13) with (C8) and Eq. (C16) with (C17) produce consistent results for  $l, n_r < 10$  and have the same behavior  $M \sim x^{1/2}$  [29].

For the light systems ( $m_1, m_2 \rightarrow 0$ ), Eq. (C1) simplifies to

$$M\Psi_{d,t}(\mathbf{r}) = [2|\mathbf{p}| + V_{d,t}] \Psi_{d,t}(\mathbf{r}). \quad (\text{C20})$$

By employing the Bohr-Sommerfeld quantization approach [61], the parameterized formula can be written as [28, 32]

$$M = \beta_x \sqrt{x + c_{0x}} \quad (x = l, n_r, L, N_r). \quad (\text{C21})$$

For the light systems, the parameters read as

$$c_c = \sqrt{\sigma'}, \quad c_{l,L} = 2\sqrt{2}, \quad c_{n_r,N_r} = 2\sqrt{\pi}. \quad (\text{C22})$$

According to the results in Refs. [42, 44], similar to Eq. (C16) [29], we suggest

$$M = C' + \sqrt{\beta_x^2(x + c_{0x}) + \kappa_x \left( m_1^{3/2} + m_2^{3/2} \right) (x + c_{0x})^{1/4}}. \quad (\text{C23})$$

Based on Eq. (C18) [67] and (C19), we obtain a modified Regge trajectory relation for the light-light systems in Ref. [46]

$$M = m_R + \beta_x \sqrt{x + c_{0x}}, \quad (\text{C24})$$

where

$$c_c = \sqrt{\sigma'}, \quad c_{l,L} = 2\sqrt{2}, \quad c_{n_r,N_r} = 2\sqrt{\pi}. \quad (\text{C25})$$

$m_R$  is in Eq. (C8) with  $m_{1,2}$  being the masses of the light constituents.

When Eq. (C13) with (C8) is employed to discuss the heavy-light systems, and Eq. (C24) with (C8) is used to discuss the light systems, summarizing Eqs. (C7), (C13) with (C8) and (C24) with (C8), we have a general form of the Regge trajectories [28, 69]

$$\begin{aligned} M &= m_R + \beta_x(x + c_{0x})^\nu \quad (x = l, n_r, L, N_r), \\ m_R &= m_1 + m_2 + C', \quad \beta_x = c_{fx}c_xc_c, \end{aligned} \quad (\text{C26})$$

TABLE XI: The coefficients for the heavy-heavy systems (HHS), the heavy-light systems (HLS), and the light-light systems (LLS).

	HHS	HLS	LLS
$\nu$	2/3	1/2	1/2
$c_c$	$(\sigma'^2/\mu)^{1/3}$	$\sqrt{\sigma'}$	$\sqrt{\sigma'}$
$c_{l, L}$	3/2	2	$2\sqrt{2}$
$c_{n_r, N_r}$	$(3\pi)^{2/3}/2$	$\sqrt{2\pi}$	$2\sqrt{\pi}$

where  $\nu$ ,  $c_x$  and  $c_c$  are listed in Table XI.  $c_{fx}$  are theoretically equal to one and are fitted in practice.  $c_{0x}$  vary with different Regge trajectories. Eq. (C26) can be employed to discuss various systems including the heavy-heavy systems, the heavy-light systems, and the light-light systems: diquarks, mesons, baryons, and tetraquarks [33, 34, 46].

It should be noticed that the general form (C26) is provisional. Because there are different methods to include the masses of the light constituents. To distinguish the better one, more theoretical and experimental data are needed. In addition to this, the parameter values are universal for both the heavy-heavy systems and the heavy-light systems [29, 47], while the parameter values should change for the light systems [46] to obtain agreeable results.

### 3. Behaviors of the Regge trajectories for various tetraquarks

The Regge trajectories behave differently in different energy regions [28, 32]. The Regge trajectory behaviors for baryons are discussed in Ref. [69]. In this subsection, we discuss the Regge trajectory behaviors for various tetraquarks.

Taken as an example, tetraquarks  $(cc)(\bar{q}\bar{q}')$  are discussed, where  $q$  and  $q'$  are the light quarks,  $u$ ,  $d$ , or  $s$ . The diquark  $(cc)$  is the doubly heavy diquark, therefore, the diquark Regge trajectories are clear, see Eq. (C7),

$$M_{\rho_1} \sim x_{\rho_1}^{2/3} \quad (x_{\rho_1} = l_1, n_{r_1}), \quad (\text{C27})$$

where  $M_{\rho_1}$  is mass of the diquark  $(cc)$ . The antidiquark  $(\bar{q}\bar{q}')$  is the light diquark. Although they have indefinite forms [see Eqs. (C23) and (C24) with (C8)], the light-diquark Regge trajectories have the same behavior,

$$M_{\rho_2} \sim x_{\rho_2}^{1/2} \quad (x_{\rho_2} = l_2, n_{r_2}), \quad (\text{C28})$$

where  $M_{\rho_2}$  is mass of the antidiquark  $(\bar{q}\bar{q}')$ . Generally speaking, the diquark Regge trajectories are not the same as the  $\rho$ -trajectories of tetraquarks.

When discussing the  $\lambda$ -mode, the Regge trajectory relation for the tetraquarks  $(cc)(\bar{q}\bar{q}')$  is not clear. We will be confronted with two problems. One is when the light antidiquark can be regarded as being heavy, which will affect not only the behaviors of the  $\lambda$ -trajectories but

also the behaviors of the  $\rho$ -trajectories. Another is how to introduce the mass of the light constituent if the antidiquark is light, which will affect the behavior of the  $\rho$ -trajectories. If the light antidiquark  $(\bar{q}\bar{q}')$  is regarded as being light, the tetraquarks  $(cc)(\bar{q}\bar{q}')$  are the heavy-light systems, therefore,  $\lambda$ -trajectories behave as

$$M \sim x_{\lambda}^{1/2} \quad (x_{\lambda} = L, N_r) \quad (\text{C29})$$

no matter whether Eq. (C13) with (C8) or Eq. (C16) with (C17) is chosen as the  $\lambda$ -trajectory formula. When Eq. (C16) is chosen as the  $\lambda$ -trajectory relation, it will give  $M \sim M_{\rho_1}, M_{\rho_2}^{3/2}$  while Eq. (C13) with (C8) gives  $M \sim M_{\rho_1}, M_{\rho_2}$  due to different ways to include the light constituent's mass  $M_{\rho_2}$  [corresponding to  $m_2$  in Eq. (C13) with (C8) and Eq. (C16) with (C17)]. They give two different behaviors of the  $\rho$ -trajectories. Using Eqs. (C27) and (C28), Eq. (C13) with (C8) gives  $M \sim x_{\rho_1}^{2/3}, x_{\rho_2}^{3/4}$  while Eq. (C16) with (C17) gives  $M \sim x_{\rho_1}^{2/3}, x_{\rho_2}^{1/2}$ . [When discussing the  $\rho$ -trajectories, highly excited antidiquarks are involved. The first radially and orbitally excited ( $ud$ ) are about 1.3 GeV. The masses of the  $1^1p_1$  states of  $(us)$  and  $(ss)$  are much heavier, 1.46 GeV and 1.65 GeV [46], respectively. They approximate or even are larger than the mass of the charm quark. Therefore, the light antidiquark can be regarded as being heavy.] If the light antidiquark is regarded as being heavy,  $\lambda$ -trajectories behave as

$$M \sim x_{\lambda}^{2/3} \quad (\text{C30})$$

according to Eq. (C7) with (C8). Using Eqs. (C7), (C8), (C27), and (C28), we have  $M \sim M_{\rho_1}, M_{\rho_2} \sim x_{\rho_1}^{2/3}, x_{\rho_2}^{1/2}$ .

Other types of tetraquarks can be discussed by similar way. The Regge trajectory behaviors of different types of tetraquarks are listed in Table XII.

When the diquark (antidiquark) is doubly heavy or heavy-light, it is clear how to introduce its large mass, see Eqs. (C7) with (C8) and Eq. (C13) with (C8) or Eq. (C16) with (C17). After choosing the Regge trajectory formulas for the heavy-light diquarks, for example, (C13) with (C8), the Regge trajectory formulas can be written explicitly, and then the behaviors of the  $\lambda$ -trajectory and the  $\rho$ -trajectory are definite. Using Eq. (C26), the Regge trajectory relations for the tetraquarks  $(Q_1 q_1)(\bar{Q}_2 \bar{q}_2)$  read

$$\begin{aligned} M &= m_{R\lambda} + \beta_{x_\lambda} (x_\lambda + c_{0x_\lambda})^{2/3} \quad (x_\lambda = L, N_r), \\ M_{\rho_1} &= m_{R\rho_1} + \beta_{x_{\rho_1}} \sqrt{x_{\rho_1} + c_{0x_{\rho_1}}} \quad (x_{\rho_1} = l_1, n_{r_1}), \\ M_{\rho_2} &= m_{R\rho_2} + \beta_{x_{\rho_2}} \sqrt{x_{\rho_2} + c_{0x_{\rho_2}}} \quad (x_{\rho_2} = l_2, n_{r_2}), \end{aligned} \quad (\text{C31})$$

TABLE XII: Behaviors of three series of Regge trajectory for different tetraquarks in the diquark picture.  $Q = c, b$  and  $q = u, d, s$ .  $M$  is the mass of the tetraquark.  $x_\lambda = L, N_r$  are the angular momentum quantum number and the radial quantum number for the  $\lambda$  mode.  $x_{\rho_1} = l_1, n_{r_1}$  are for the  $\rho_1$  mode and  $x_{\rho_2} = l_2, n_{r_2}$  are for the  $\rho_2$  mode.  $?$  denotes the indefinite result.

	Trajectory behavior $M \sim x^\nu$			Trajectory behavior $M^2 \sim x^\nu$		
	$\rho_1$ -mode	$\rho_2$ -mode	$\lambda$ -mode	$\rho_1$ -mode	$\rho_2$ -mode	$\lambda$ -mode
1	$(q_1 q'_1)(\bar{q}_2 \bar{q}'_2)$	$x_{\rho_1}^{1/2} ?, x_{\rho_1}^{3/4} ?$	$x_{\rho_2}^{1/2} ?, x_{\rho_2}^{3/4} ?$	$x_\lambda^{1/2} ?, x_\lambda^{2/3} ?$	$x_{\rho_1}^{1/2} ?, x_{\rho_1}^{3/4} ?$	$x_{\rho_2}^{1/2} ?, x_{\rho_2}^{3/4} ?$
2	$(q_1 q'_1)(\bar{Q}_2 \bar{q}_2)$	$x_{\rho_1}^{1/2} ?, x_{\rho_1}^{3/4} ?$	$x_{\rho_2}^{1/2}$	$x_\lambda^{1/2} ?, x_\lambda^{2/3} ?$	$x_{\rho_1}^{1/2} ?, x_{\rho_1}^{3/4} ?$	$x_{\rho_2}^{1/2}$
3	$(q_1 Q_1)(\bar{q}_2 \bar{q}'_2)$	$x_{\rho_1}^{1/2}$	$x_{\rho_2}^{1/2} ?, x_{\rho_2}^{3/4} ?$	$x_\lambda^{1/2} ?, x_\lambda^{2/3} ?$	$x_{\rho_1}^{1/2}$	$x_{\lambda}^{1/2} ?, x_{\lambda}^{2/3} ?$
4	$(q_1 q'_1)(\bar{Q}_2 \bar{Q}'_2)$	$x_{\rho_1}^{1/2} ?, x_{\rho_1}^{3/4} ?$	$x_{\rho_2}^{2/3}$	$x_\lambda^{1/2} ?, x_\lambda^{2/3} ?$	$x_{\rho_1}^{1/2} ?, x_{\rho_1}^{3/4} ?$	$x_{\rho_2}^{2/3}$
5	$(Q_1 Q'_1)(\bar{q}_2 \bar{q}'_2)$	$x_{\rho_1}^{2/3}$	$x_{\rho_2}^{1/2} ?, x_{\rho_2}^{3/4} ?$	$x_\lambda^{1/2} ?, x_\lambda^{2/3} ?$	$x_{\rho_1}^{2/3}$	$x_{\rho_2}^{1/2} ?, x_{\rho_2}^{3/4} ?$
6	$(q_1 Q_1)(\bar{Q}_2 \bar{q}_2)$	$x_{\rho_1}^{1/2}$	$x_{\rho_2}^{1/2}$	$x_\lambda^{2/3}$	$x_{\rho_1}^{1/2}$	$x_\lambda^{2/3}$
7	$(q_1 Q_1)(\bar{Q}_2 \bar{Q}'_2)$	$x_{\rho_1}^{1/2}$	$x_{\rho_2}^{2/3}$	$x_\lambda^{2/3}$	$x_{\rho_1}^{1/2}$	$x_\lambda^{2/3}$
8	$(Q_1 Q'_1)(\bar{Q}_2 \bar{q}_2)$	$x_{\rho_1}^{2/3}$	$x_{\rho_2}^{1/2}$	$x_\lambda^{2/3}$	$x_{\rho_1}^{2/3}$	$x_\lambda^{2/3}$
9	$(Q_1 Q'_1)(\bar{Q}_2 \bar{Q}'_2)$	$x_{\rho_1}^{2/3}$	$x_{\rho_2}^{2/3}$	$x_\lambda^{2/3}$	$x_{\rho_1}^{2/3}$	$x_\lambda^{2/3}$

where

where

$$\begin{aligned}
 m_{R\lambda} &= M_{\rho_1} + M_{\rho_2} + C, \\
 m_{R\rho_1} &= M_{Q_1} + m_{q_1} + C/2, \\
 m_{R\rho_2} &= M_{Q_2} + m_{q_2} + C/2, \\
 \beta_L &= \frac{3}{2} \left( \frac{\sigma^2}{\mu_\lambda} \right)^{1/3} c_{fL}, \\
 \beta_{N_r} &= \frac{(3\pi)^{2/3}}{2} \left( \frac{\sigma^2}{\mu_\lambda} \right)^{1/3} c_{fN_r}, \\
 \mu_\lambda &= \frac{M_{\rho_1} M_{\rho_2}}{M_{\rho_1} + M_{\rho_2}}, \quad \mu_{\rho_1} = \frac{m_{Q_1} m_{Q'_1}}{m_{Q_1} + m_{Q'_1}}, \\
 \beta_{l_1} &= \sqrt{2\sigma} c_{fl_1}, \quad \beta_{n_{r_1}} = \sqrt{\pi\sigma} c_{fn_{r_1}}, \\
 \beta_{l_2} &= \sqrt{2\sigma} c_{fl_2}, \quad \beta_{n_{r_2}} = \sqrt{\pi\sigma} c_{fn_{r_2}}. \tag{C32}
 \end{aligned}$$

$$\begin{aligned}
 m_{R\lambda} &= M_{\rho_1} + M_{\rho_2} + C, \\
 m_{R\rho_1} &= m_{Q_1} + m_{Q'_1} + C/2, \\
 m_{R\rho_2} &= m_{Q_2} + m_{q_2} + C/2, \\
 \beta_L &= \frac{3}{2} \left( \frac{\sigma^2}{\mu_\lambda} \right)^{1/3} c_{fL}, \quad \beta_{N_r} = \frac{(3\pi)^{2/3}}{2} \left( \frac{\sigma^2}{\mu_\lambda} \right)^{1/3} c_{fN_r}, \\
 \mu_\lambda &= \frac{M_{\rho_1} M_{\rho_2}}{M_{\rho_1} + M_{\rho_2}}, \quad \mu_{\rho_1} = \frac{m_{Q_1} m_{Q'_1}}{m_{Q_1} + m_{Q'_1}}, \\
 \beta_{l_1} &= \frac{3}{2} \left( \frac{\sigma^2}{4\mu_{\rho_1}} \right)^{1/3} c_{fl_1}, \quad \beta_{l_2} = \sqrt{2\sigma} c_{fl_2}, \\
 \beta_{n_{r_1}} &= \frac{(3\pi)^{2/3}}{2} \left( \frac{\sigma^2}{4\mu_{\rho_1}} \right)^{1/3} c_{fn_{r_1}}, \quad \beta_{n_{r_2}} = \sqrt{\pi\sigma} c_{fn_{r_2}}. \tag{C34}
 \end{aligned}$$

The Regge trajectory relations for the tetraquarks  $(Q_1 Q'_1)(\bar{Q}_2 \bar{q}_2)$  read

The tetraquark Regge trajectory relations for  $(Q_1 q_1)(\bar{Q}_2 \bar{Q}'_2)$  can be obtained easily by the similar way as obtaining the Regge trajectory formulas for  $(Q_1 Q'_1)(\bar{Q}_2 \bar{q}_2)$ . The Regge trajectory relations for the tetraquarks  $(Q_1 Q'_1)(\bar{Q}_2 \bar{Q}'_2)$  read

$$\begin{aligned}
 M &= m_{R\lambda} + \beta_{x_\lambda} (x_\lambda + c_{0x_\lambda})^{2/3} \quad (x_\lambda = L, N_r), \\
 M_{\rho_1} &= m_{R\rho_1} + \beta_{x_{\rho_1}} (x_{\rho_1} + c_{0x_{\rho_1}})^{2/3} \quad (x_{\rho_1} = l_1, n_{r_1}), \\
 M_{\rho_2} &= m_{R\rho_2} + \beta_{x_{\rho_2}} \sqrt{x_{\rho_2} + c_{0x_{\rho_2}}} \quad (x_{\rho_2} = l_2, n_{r_2}), \tag{C33}
 \end{aligned}$$

$$\begin{aligned}
 M &= m_{R\lambda} + \beta_{x_\lambda} (x_\lambda + c_{0x_\lambda})^{2/3} \quad (x_\lambda = L, N_r), \\
 M_{\rho_1} &= m_{R\rho_1} + \beta_{x_{\rho_1}} (x_{\rho_1} + c_{0x_{\rho_1}})^{2/3} \quad (x_{\rho_1} = l_1, n_{r_1}), \\
 M_{\rho_2} &= m_{R\rho_2} + \beta_{x_{\rho_2}} (x_{\rho_2} + c_{0x_{\rho_2}})^{2/3} \quad (x_{\rho_2} = l_2, n_{r_2}), \tag{C35}
 \end{aligned}$$

where

$$\begin{aligned}
m_{R\lambda} &= M_{\rho_1} + M_{\rho_2} + C, \\
m_{R\rho_1} &= m_{Q_1} + m_{Q'_1} + C/2, \\
m_{R\rho_2} &= m_{Q_2} + m_{Q'_2} + C/2, \\
\beta_L &= \frac{3}{2} \left( \frac{\sigma^2}{\mu_\lambda} \right)^{1/3} c_{fL}, \quad \beta_{N_r} = \frac{(3\pi)^{2/3}}{2} \left( \frac{\sigma^2}{\mu_\lambda} \right)^{1/3} c_{fN_r}, \\
\mu_\lambda &= \frac{M_{\rho_1} M_{\rho_2}}{M_{\rho_1} + M_{\rho_2}}, \quad \mu_{\rho_1} = \frac{m_{Q_1} m_{Q'_1}}{m_{Q_1} + m_{Q'_1}}, \\
\mu_{\rho_2} &= \frac{m_{Q_2} m_{Q'_2}}{m_{Q_2} + m_{Q'_2}}, \quad \beta_{l_1} = \frac{3}{2} \left( \frac{\sigma^2}{4\mu_{\rho_1}} \right)^{1/3} c_{fl_1}, \\
\beta_{n_{r_1}} &= \frac{(3\pi)^{2/3}}{2} \left( \frac{\sigma^2}{4\mu_{\rho_1}} \right)^{1/3} c_{fn_{r_1}}, \\
\beta_{l_2} &= \frac{3}{2} \left( \frac{\sigma^2}{4\mu_{\rho_2}} \right)^{1/3} c_{fl_2}, \\
\beta_{n_{r_2}} &= \frac{(3\pi)^{2/3}}{2} \left( \frac{\sigma^2}{4\mu_{\rho_2}} \right)^{1/3} c_{fn_{r_2}}. \tag{C36}
\end{aligned}$$

Due to ambiguity, the tetraquark Regge trajectory formulas for the tetraquarks containing the light diquark or the light antiquark are not given.

#### 4. Discussions

The form of the Regge trajectories depends not only on energy regions but also on the confining potential [28, 32]. In this work, the employed confining potential is linear. Moreover, various mixings are not considered when discussing the behaviors of the tetraquark Regge trajectories, see Table XII. When the mixings are considered, the behaviors of the tetraquark Regge trajectories will become complex.

In potential models, the curvature of the Regge trajectories is related to the dynamic equation and the confining potential [70]. In Ref. [33], we suggest that the Regge trajectories for the diquarks, mesons, baryons and tetraquarks are concave downward in the  $(M^2, x)$  planes. In fact, the baryon trajectories and the tetraquark Regge trajectories discussed in Refs. [33, 34] actually are the  $\lambda$ -trajectories. We can see from Table XII that both the  $\lambda$ -trajectories and the  $\rho$ -trajectories for various tetraquarks are all concave downward in the  $(M^2, x)$  plane. For the light systems, the trajectories approximate linear as the masses are neglected and become concave when the masses are considered.

If the diquark quark contents have the same flavors as the antiquark contents, there are degeneracy in masses. The  $\rho_1$ -mode excited states have the same masses as the  $\rho_2$ -mode excited states.

#### Appendix D: Determination of $c_{fx_\lambda}$ and $c_{0x_\lambda}$ for the $\lambda$ -modes

In this section, we determine the values of  $c_{fx_\lambda}$  and  $c_{0x_\lambda}$  for the  $\lambda$ -modes of the tetraquarks with hidden bottom and charm. Apply Eq. (C26) to fit the Regge trajectories for the doubly heavy mesons, the  $\lambda$ -modes of heavy-heavy baryons composed of one heavy quark and one doubly heavy (or one heavy-light) diquark and the  $\lambda$ -modes of heavy-heavy tetraquarks composed of one doubly heavy (or heavy-light) diquark and one doubly heavy (or heavy-light) antiquark. The quality of a fit is measured by the quantity  $\chi^2$  defined by

$$\chi^2 = \frac{1}{N-1} \sum_{i=1}^N \left( \frac{M_{fi} - M_{ei}}{M_{ei}} \right)^2, \tag{D1}$$

where  $N$  is the number of points on the trajectory,  $M_{fi}$  is fitted value and  $M_{ei}$  is the experimental value or the theoretical value of the  $i$ -th particle mass. The parameters are determined by minimizing  $\chi^2$ .

TABLE XIII: The spin averaged masses of the radially excited states of mesons and baryons, and the masses of tetraquarks (in GeV).

	$1S$	$2S$	$3S$	$4S$	$5S$	$6S$
$c\bar{c}$	3.0687	3.6740	4.0273	4.4115	4.8305	5.1640
$c\bar{b}$	6.3184	6.8793	7.2500	7.6030	7.9430	
$b\bar{b}$	9.4450	10.0173	10.3486	10.5778	10.8645	11.0812
$\Omega_{ccb}$	7.9940	8.4097				
$\Omega_{cbb}$	11.2107	11.6967				
$[cs][\bar{c}\bar{s}]$	4.051	4.604				
$[bs][\bar{b}\bar{s}]$	10.662	11.111				

TABLE XIV: The spin averaged masses of the orbitally excited states of mesons and baryons, and the masses of tetraquarks (in GeV).

	$1S$	$1P$	$1D$	$1F$	$1G$	$1H$
$c\bar{c}$	3.0687	3.5253	3.8186	4.0720	4.3435	4.5931
$c\bar{b}$	6.3184	6.7486	7.0261	7.2720	7.4879	
$b\bar{b}$	9.4450	9.8997	10.1629	10.3467	10.5127	10.6711
$\Omega_{ccb}$	7.9940	8.2643	8.4741			
$\Omega_{cbb}$	11.2107	11.5261	11.8053			
$[cs][\bar{c}\bar{s}]$	4.051	4.466	4.728			
$[bs][\bar{b}\bar{s}]$	10.662	11.002	11.216			

The masses used are listed in Tables XIII and XIV. For the mesons and baryons, the listed data are the spin averaged masses. If the corresponding states are experimentally determined, the PDG data from Ref. [3] are used. For the undetermined states, the theoretical data from Ref. [71, 72] are used. (In Ref. [72], the mass of the  $\Omega_{cbb}(7/2)^+(1D)$  state is not provided, so we use the value 11.807 GeV.) The theoretical data for the tetraquarks are from [10, 73]. Beside the bound states' masses, some

parameters are listed in Table I. The masses of the axial vector diquarks are  $m_{\{cc\}} = 3.14$  GeV,  $m_{\{bb\}} = 9.63$  GeV [47]. The masses of the scalar diquarks [cs] and [bs] are calculated by using the parameters in Table I and Eq. (C26) or (C31) [29].

The fitted parameters are listed in Table XV. The fitted Regge trajectories are plotted in the  $((M - m_R)^{3/2}, x)$  plane, see Fig. 6. The results are consistent with those in Ref. [34].

The fitted  $c_{fx_\lambda}$  and  $c_{0x_\lambda}$  vary across different Regge trajectories for different states and for different systems, see Fig. 7 and Table XV. In case of the baryons and tetraquarks, these parameters are sensitive to diquark masses. For example,  $c_{fN_r} = 1.218$  when  $[bc] = 6.38$  GeV [47] while  $c_{fN_r} = 1.027$  when  $[bc] = 6.519$  GeV, as determined by fitting the radial Regge trajectory for the tetraquark  $[bc][\bar{b}\bar{c}]$  [73].

According to Eq. (C31),  $c_{fx_\lambda}$  and  $c_{0x_\lambda}$  are needed to determine a Regge trajectory as  $m_{R_\lambda}$  can be calculated by using Eq. (C32) and parameters in Table I. Two or more states on the Regge trajectory are needed to obtain  $c_{fx_\lambda}$  and  $c_{0x_\lambda}$ . We choose  $c_{fx_\lambda}$  and  $c_{0x_\lambda}$  by fitting these parameters from other systems. By fitting the data in Table XV, we have

$$c_{fL} = 1.116 + 0.013\mu_\lambda, \quad c_{0L} = 0.540 - 0.141\mu_\lambda, \quad (D2)$$

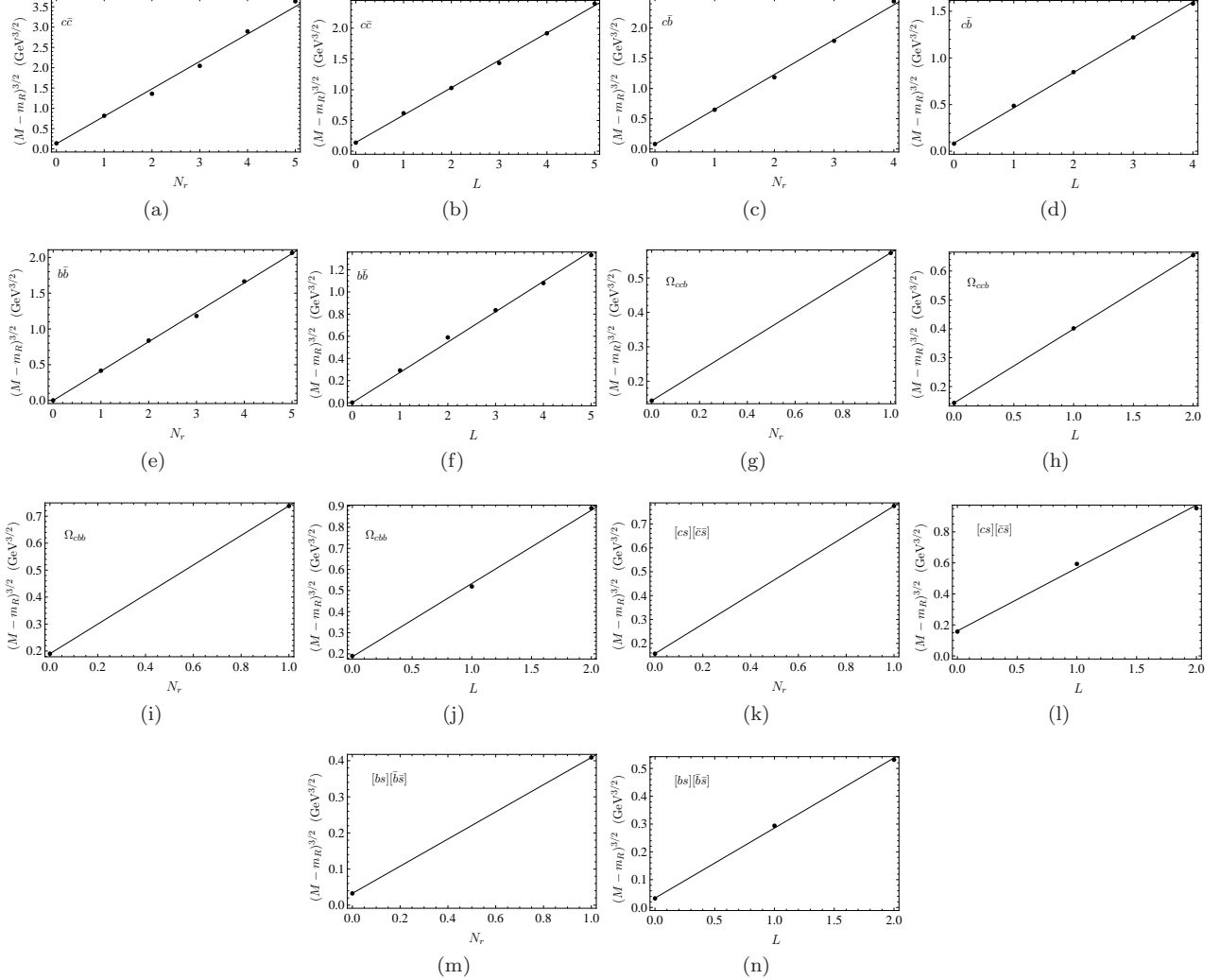
$$c_{fN_r} = 1.008 + 0.008\mu_\lambda, \quad c_{0N_r} = 0.334 - 0.087\mu_\lambda \quad (D3)$$

where  $\mu_\lambda$  is the reduced masses, see Eq. (C6) or (C32). Eqs. (D2) and (D3) are obtained when  $\mu_\lambda < 3.83$  GeV. And the formulas for the  $\mu_\lambda > 3.83$  GeV are not considered here. As more experimental data or more theoretical data become available, the fitted formulas will be refined.

- 
- [1] R. L. Jaffe, Phys. Rev. D **15**, 267 (1977) doi:10.1103/PhysRevD.15.267
- [2] R. L. Jaffe, Phys. Rev. D **15**, 281 (1977) doi:10.1103/PhysRevD.15.281
- [3] S. Navas et al. (Particle Data Group), Phys. Rev. D 110, 030001 (2024)
- [4] P. Bicudo, Phys. Rept. **1039**, 1-49 (2023) doi:10.1016/j.physrep.2023.10.001 [arXiv:2212.07793 [hep-lat]].
- [5] Y. R. Liu, H. X. Chen, W. Chen, X. Liu and S. L. Zhu, Prog. Part. Nucl. Phys. **107** (2019), 237-320 doi:10.1016/j.ppnp.2019.04.003 [arXiv:1903.11976 [hep-ph]].
- [6] F. Gross, E. Klemp, S. J. Brodsky, A. J. Buras, V. D. Burkert, G. Heinrich, K. Jakobs, C. A. Meyer, K. Orginos and M. Strickland, *et al.* Eur. Phys. J. C **83**, 1125 (2023) doi:10.1140/epjc/s10052-023-11949-2 [arXiv:2212.11107 [hep-ph]].
- [7] R. L. Jaffe, Phys. Rept. **409**, 1-45 (2005) doi:10.1016/j.physrep.2004.11.005 [arXiv:hep-ph/0409065 [hep-ph]].
- [8] A. Esposito, A. Pilloni and A. D. Polosa, Phys. Rept. **668** (2017), 1-97 doi:10.1016/j.physrep.2016.11.002 [arXiv:1611.07920 [hep-ph]].
- [9] D. Ebert, R. N. Faustov and V. O. Galkin, Mod. Phys. Lett. A **24**, 567-573 (2009) doi:10.1142/S0217732309030357 [arXiv:0812.3477 [hep-ph]].
- [10] R. N. Faustov, V. O. Galkin and E. M. Savchenko, Universe **7**, no.4, 94 (2021) doi:10.3390/universe7040094 [arXiv:2103.01763 [hep-ph]].
- [11] D. Ebert, R. N. Faustov and V. O. Galkin, Eur. Phys. J. C **58**, 399-405 (2008) doi:10.1140/epjc/s10052-008-0754-8 [arXiv:0808.3912 [hep-ph]].
- [12] R. Tiwari and A. K. Rai, Few Body Syst. **64**, no.2, 20 (2023) doi:10.1007/s00601-023-01805-0 [arXiv:2206.04478 [hep-ph]].
- [13] P. Lundhammar and T. Ohlsson, Phys. Rev. D **102**, no.5, 054018 (2020) doi:10.1103/PhysRevD.102.054018 [arXiv:2006.09393 [hep-ph]].
- [14] J. Ferretti and E. Santopinto, JHEP **04**, 119 (2020) doi:10.1007/JHEP04(2020)119 [arXiv:2001.01067 [hep-ph]].
- [15] F. Giannuzzi, Nuovo Cimento Soc. Ital. Fis. C **47**, 183 (2024) [arXiv:2311.05163 [hep-ph]].
- [16] J. Hoffer, G. Eichmann and C. S. Fischer, Phys. Rev. D **109**, no.7, 074025 (2024) doi:10.1103/PhysRevD.109.074025 [arXiv:2402.12830 [hep-ph]].
- [17] J. F. Giron and R. F. Lebed, Phys. Rev. D **102**, no.1, 014036 (2020) doi:10.1103/PhysRevD.102.014036 [arXiv:2005.07100 [hep-ph]].
- [18] J. F. Giron, R. F. Lebed and S. R. Martinez, Phys. Rev. D **104**, no.5, 054001 (2021) doi:10.1103/PhysRevD.104.054001 [arXiv:2106.05883 [hep-ph]].
- [19] J. F. Giron and R. F. Lebed, Phys. Rev. D **101**, no.7, 074032 (2020) doi:10.1103/PhysRevD.101.074032 [arXiv:2003.02802 [hep-ph]].
- [20] R. F. Lebed and S. R. Martinez, Phys. Rev. D **110**, no.3, 034033 (2024) doi:10.1103/PhysRevD.110.034033 [arXiv:2406.08690 [hep-ph]].
- [21] M. R. Hadizadeh and A. Khaledi-Nasab, Phys. Lett. B **753**, 8-12 (2016) doi:10.1016/j.physletb.2015.11.072 [arXiv:1511.08542 [hep-ph]].
- [22] J. Wu, X. Liu, Y. R. Liu and S. L. Zhu, Phys. Rev. D **99**, no.1, 014037 (2019) doi:10.1103/PhysRevD.99.014037 [arXiv:1810.06886 [hep-ph]].
- [23] X.J. Liu, D.Y. Chen, H.X. Huang, J.L. Ping, X.Y. Chen, and Y.C. Yang, Sci. China Phys. Mech. Astron. **66**, no.2, 221012 (2023) doi:10.1007/s11433-022-1987-5 [arXiv:2204.08104 [hep-ph]].
- [24] W. Chen, H. X. Chen, X. Liu, T. G. Steele and S. L. Zhu, Phys. Rev. D **96**, no.11, 114017 (2017) doi:10.1103/PhysRevD.96.114017 [arXiv:1706.09731 [hep-ph]].
- [25] Z. G. Wang, Eur. Phys. J. C **79**, no.6, 489 (2019) doi:10.1140/epjc/s10052-019-7019-6 [arXiv:1903.10895 [hep-ph]].
- [26] S. M. Gerasyuta and V. I. Kochkin, [arXiv:0812.0315 [hep-ph]].
- [27] L. Maiani, F. Piccinini, A. D. Polosa and

TABLE XV: The fitted  $c_{fx\lambda}$  and  $c_{0x\lambda}$ .

	$cc$	$cb$	$bb$	$\Omega_{ccb}$	$\Omega_{cbb}$	$[cs][\bar{c}\bar{s}]$	$[bs][\bar{b}\bar{s}]$
$(c_{fN_r}, c_{0N_r})$	(0.994, 0.191)	(1.028, 0.135)	(1.046, 0.0)	(0.994, 0.333)	(1.037, 0.347)	(1.025, 0.255)	(1.022, 0.087)
$(c_{fL}, c_{0L})$	(1.120, 0.320)	(1.154, 0.231)	(1.187, 0.0)	(1.047, 0.559)	(1.137, 0.537)	(1.151, 0.399)	(1.164, 0.133)

FIG. 6: The radial and orbital Regge trajectories (the black lines) for mesons, baryons and tetraquarks. The dots are the spin averaged masses of mesons and baryons and the masses of tetraquarks.  $N_r$  and  $L$  are the radial and orbital quantum numbers for the  $\lambda$ -mode, respectively. The used data are listed in Tables XIII-XV.

- V. Riquer, Phys. Rev. D **71**, 014028 (2005) doi:10.1103/PhysRevD.71.014028 [arXiv:hep-ph/0412098 [hep-ph]].
- [28] J. K. Chen, Nucl. Phys. B **983**, 115911 (2022) doi:10.1016/j.nuclphysb.2022.115911 [arXiv:2203.02981 [hep-ph]].
- [29] J. K. Chen, X. Feng and J. Q. Xie, JHEP **10**, 052 (2023) doi:10.1007/JHEP10(2023)052 [arXiv:2308.02289 [hep-ph]].
- [30] T. J. Burns, F. Piccinini, A. D. Polosa and C. Sabelli, Phys. Rev. D **82**, 074003 (2010) doi:10.1103/PhysRevD.82.074003 [arXiv:1008.0018 [hep-ph]].
- [31] J. K. Chen, Eur. Phys. J. C **78**, no.8, 648 (2018) doi:10.1140/epjc/s10052-018-6134-0
- [32] J. K. Chen, Eur. Phys. J. A **57**, 238 (2021) doi:10.1140/epja/s10050-021-00502-y [arXiv:2102.07993 [hep-ph]].
- [33] J. K. Chen, Eur. Phys. J. C **84**, no.4, 356 (2024) doi:10.1140/epjc/s10052-024-12706-9 [arXiv:2302.06794 [hep-ph]].
- [34] J. K. Chen, Nucl. Phys. A **1050**, 122927 (2024) doi:10.1016/j.nuclphysa.2024.122927 [arXiv:2302.05926 [hep-ph]].
- [35] T. Regge, Nuovo Cim. **14**, 951 (1959)
- [36] G. F. Chew and S. C. Frautschi, Phys. Rev. Lett. **7**, 394-

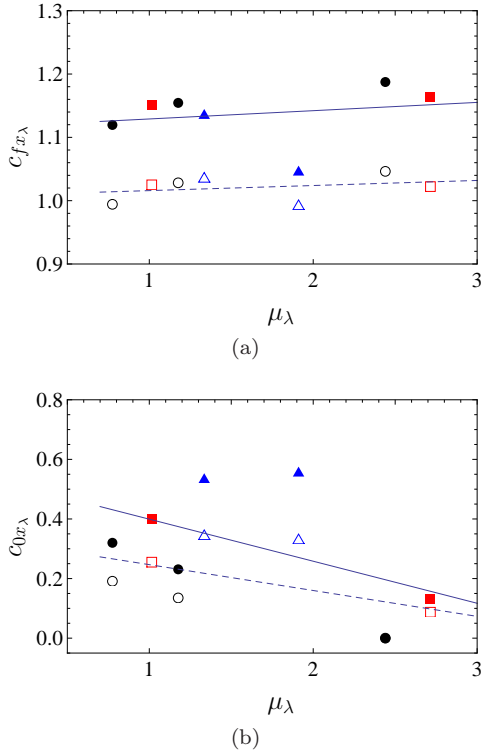


FIG. 7: The fitted  $c_{fx_\lambda}$  [Fig. 7(a)] and  $c_{0x_\lambda}$  [Fig. 7(b)]. The data are listed in Table XV.  $\mu_\lambda$  is the reduced masses, see Eq. (C6) or (C32). The black filled circles (mesons), the red filled squares (tetraquarks), and the green filled triangles (baryons) are the fitted  $c_{fL}$  or  $c_{0L}$ . The black empty circles (mesons), the red empty squares (tetraquarks), and the green empty triangles (baryons) are the fitted  $c_{fN_r}$  or  $c_{0N_r}$ . The black lines ( $c_{fL}$  and  $c_{0L}$ ) and the dashed lines ( $c_{fN_r}$  and  $c_{0N_r}$ ) are the linear fit, see Eqs. (D2) and (D3).

- 397 (1961) doi:10.1103/PhysRevLett.7.394
- [37] G. F. Chew and S. C. Frautschi, Phys. Rev. Lett. **8**, 41 (1962)
- [38] Y. Nambu, Phys. Lett. B **80**, 372 (1979)
- [39] P. D. B. Collins, Phys. Rept. **1**, 103 (1971);
- [40] A. Inopin and G. S. Sharov, Phys. Rev. D **63**, 054023 (2001). arXiv: hep-ph/9905499.
- [41] A. C. Irving and R. P. Worden, Phys. Rept. **34**, 117 (1977)
- [42] A. Selem and F. Wilczek, in New Trends in HERA Physics 2005 (World Scientific, Singapore, 2006), pp. 337-356 doi:10.1142/9789812773524\_0030 [arXiv:hep-ph/0602128 [hep-ph]].
- [43] M. Nielsen and S. J. Brodsky, Phys. Rev. D **97**, no.11, 114001 (2018) doi:10.1103/PhysRevD.97.114001 [arXiv:1802.09652 [hep-ph]].
- [44] J. Sonnenschein and D. Weissman, Eur. Phys. J. C **79**, no.4, 326 (2019) doi:10.1140/epjc/s10052-019-6828-y [arXiv:1812.01619 [hep-ph]].
- [45] M. A. Martin Contreras and A. Vega, Phys. Rev. D **102**, no.4, 046007 (2020) doi:10.1103/PhysRevD.102.046007 [arXiv:2004.10286 [hep-ph]].
- [46] J. K. Chen, J. Q. Xie, X. Feng and H. Song, Eur. Phys. J. C **83**, no.12, 1133 (2023) doi:10.1140/epjc/s10052-023-12329-6 [arXiv:2310.05131 [hep-ph]].
- [47] X. Feng, J. K. Chen and J. Q. Xie, Phys. Rev. D **108**, no.3, 034022 (2023) doi:10.1103/PhysRevD.108.034022 [arXiv:2305.15705 [hep-ph]].
- [48] L. Zhang, X. W. Kang and X. H. Guo, Eur. Phys. J. C **82**, no.4, 375 (2022) doi:10.1140/epjc/s10052-022-10332-x [arXiv:2203.02301 [hep-ph]].
- [49] S. Navas *et al.* [Particle Data Group], Phys. Rev. D **110**, no.3, 030001 (2024) doi:10.1103/PhysRevD.110.030001
- [50] M. A. Bedolla, J. Ferretti, C. D. Roberts and E. Santopinto, Eur. Phys. J. C **80**, no.11, 1004 (2020) doi:10.1140/epjc/s10052-020-08579-3 [arXiv:1911.00960 [hep-ph]].
- [51] J. Ferretti, Few Body Syst. **60**, no.1, 17 (2019) doi:10.1007/s00601-019-1483-2
- [52] S. Godfrey and N. Isgur, Phys. Rev. D **32**, 189-231 (1985) doi:10.1103/PhysRevD.32.189
- [53] B. Durand and L. Durand, Phys. Rev. D **25**, 2312 (1982) doi:10.1103/PhysRevD.25.2312
- [54] B. Durand and L. Durand, Phys. Rev. D **30**, 1904 (1984) doi:10.1103/PhysRevD.30.1904
- [55] D. B. Lichtenberg, W. Namgung, E. Predazzi and J. G. Wills, Phys. Rev. Lett. **48**, 1653 (1982) doi:10.1103/PhysRevLett.48.1653
- [56] S. Jacobs, M. G. Olsson and C. Suchyta, III, Phys. Rev. D **33**, 3338 (1986) [erratum: Phys. Rev. D **34**, 3536 (1986)] doi:10.1103/PhysRevD.33.3338
- [57] J. Ferretti, A. Vassallo and E. Santopinto, Phys. Rev. C **83**, 065204 (2011) doi:10.1103/PhysRevC.83.065204
- [58] E. Eichten, K. Gottfried, T. Kinoshita, J. B. Kogut, K. D. Lane and T. M. Yan, Phys. Rev. Lett. **34**, 369-372 (1975) [erratum: Phys. Rev. Lett. **36**, 1276 (1976)] doi:10.1103/PhysRevLett.34.369
- [59] W. Lucha, F. F. Schoberl and D. Gromes, Phys. Rept. **200**, 127-240 (1991) doi:10.1016/0370-1573(91)90001-3
- [60] D. Gromes, Z. Phys. C **11**, 147 (1981) doi:10.1007/BF01573997
- [61] F. Brau, Phys. Rev. D **62**, 014005 (2000) doi:10.1103/PhysRevD.62.014005 [arXiv:hep-ph/0412170 [hep-ph]].
- [62] S. Veseli and M. G. Olsson, Phys. Lett. B **383**, 109-115 (1996) doi:10.1016/0370-2693(96)00721-6 [arXiv:hep-ph/9606257 [hep-ph]].
- [63] P. Jakhad, J. Oudichhya, K. Gandhi and A. K. Rai, Phys. Rev. D **108**, no.1, 014011 (2023) doi:10.1103/PhysRevD.108.014011 [arXiv:2306.06349 [hep-ph]].
- [64] B. Chen, K.W. Wei, and A.L. Zhang, Eur. Phys. J. A **51**, 82 (2015) doi:10.1140/epja/i2015-15082-3 [arXiv:1406.6561 [hep-ph]].
- [65] K. Chen, Y.B. Dong, X. Liu, Q.F. Lü, and T. Matsuki, Eur. Phys. J. C **78**, no.1, 20 (2018) doi:10.1140/epjc/s10052-017-5512-3 [arXiv:1709.07196 [hep-ph]].
- [66] D.J. Jia and W.C. Dong, Eur. Phys. J. Plus **134**, no.3, 123 (2019) doi:10.1140/epjp/i2019-12474-8 [arXiv:1811.04214 [hep-ph]].
- [67] S. S. Afonin and I. V. Pusenkov, Phys. Rev. D **90**, no.9, 094020 (2014) doi:10.1103/PhysRevD.90.094020 [arXiv:1411.2390 [hep-ph]].
- [68] M. N. Sergeenko, Z. Phys. C **64**, 315-322 (1994) doi:10.1007/BF01557404
- [69] J. Q. Xie, H. Song, and J. K. Chen, Eur. Phys. J. C **84**, 1048 (2024), [arXiv:2407.18280 [hep-ph]].

- [70] J. K. Chen, Phys. Lett. B **786**, 477-484 (2018) doi:10.1016/j.physletb.2018.10.022 [arXiv:1807.11003 [hep-ph]].
- [71] R. N. Faustov and V. O. Galkin, Phys. Rev. D **105**, no.1, 014013 (2022) doi:10.1103/PhysRevD.105.014013 [arXiv:2111.07702 [hep-ph]].
- [72] D. Ebert, R. N. Faustov and V. O. Galkin, Eur. Phys. J. C **71**, 1825 (2011) doi:10.1140/epjc/s10052-011-1825-9 [arXiv:1111.0454 [hep-ph]].
- [73] R. N. Faustov, V. O. Galkin and E. M. Savchenko, Symmetry **14**, no.12, 2504 (2022) doi:10.3390/sym14122504 [arXiv:2210.16015 [hep-ph]].